

Received 28 January 2024, accepted 20 February 2024, date of publication 26 February 2024, date of current version 4 March 2024.

Digital Object Identifier 10.1109/ACCESS.2024.3370238



RESEARCH ARTICLE

Empowering Glioma Prognosis With Transparent Machine Learning and Interpretative Insights Using Explainable AI

ANISHA PALKAR^{ID1}, CIFHA CRECIL DIAS^{ID1}, (Senior Member, IEEE), KRISHNARAJ CHADAGA^{ID2}, AND NIRANJANA SAMPATHILA^{ID1}, (Senior Member, IEEE)

¹Department of Biomedical Engineering, Manipal Institute of Technology, Manipal Academy of Higher Education, Manipal 576104, India

²Department of Computer Science and Engineering, Manipal Institute of Technology, Manipal Academy of Higher Education, Manipal 576104, India

Corresponding authors: Cifha Crecil Dias (cifha.saldanha@manipal.edu) and Niranjana Sampathila (niranjana.s@manipal.edu)

ABSTRACT The primary objective of this research is to create a reliable technique to determine whether a patient has glioma, a specific kind of brain tumour, by examining various diagnostic markers, using a variety of machine learning as well as deep learning approaches, and involving XAI (explainable artificial intelligence) methods. Through the integration of patient data, including medical records, genetic profiles, algorithms using machine learning have the ability to predict how each individual will react to different medical interventions. To guarantee regulatory compliance and inspire confidence in AI-driven healthcare solutions, XAI is incorporated. Machine learning methods employed in this study includes Random Forest, decision trees, logistic regression, KNN, Adaboost, SVM, Catboost, LGBM classifier, and Xgboost whereas the deep learning methods include ANN and CNN. Four alternative XAI strategies, including SHAP, Eli5, LIME, and QLattice algorithm, are employed to comprehend the predictions of the model. The Xgboost, a ML model achieved accuracy, precision, recall, f1 score, and AUC of 88%, 82%, 94%, 88%, and 92%, respectively. The best characteristics according to XAI techniques are IDH1, Age at diagnosis, PIK3CA, ATRX, PTEN, CIC, EGFR and TP53. By applying data analytic techniques, the objective is to provide healthcare professionals with practical tool that enhances their capacity for decision-making, enhances resource management, and ultimately raises the bar for patient care. Medical experts can customise treatments and improve patient outcomes by taking into account patient's particular characteristics. XAI provides justifications to foster faith amongst patients and medical professionals who must rely on AI-assisted diagnosis and treatment recommendations.

INDEX TERMS Glioma, molecular makeup, explainable artificial intelligence (XAI), SHAP, LIME, QLattice, Eli5, machine learning.

I. INTRODUCTION

The most typical kind of Central nervous system cancer which arises from glial cells is called glioma [1]. One kind of brain cancer that penetrates the outer layer of the brain is glioma. Glioblastoma is the most malignant type of tumours [1]. Gliomas are growths of cells that start in the brain or spinal cord. Healthy brain cells called glial cells mimic the cells found in gliomas. By encircling nerve cells,

The associate editor coordinating the review of this manuscript and approving it for publication was Nuno M. Garcia .

glial cells facilitate their functionality. When a glioma grows, a clump of cells called a tumour forms [2]. The tumour can expand to the point that it presses against brain or the spinal cord, causing signs and symptoms. The symptoms depend on the precise region of the brain or the spinal cord that is impacted. Malignant gliomas can enter healthy brain tissue and grow swiftly. Treatment options for gliomas generally involve surgery, radiation therapy, chemotherapy, and other treatments. Depending on where the glioma is, different symptoms could be present. The type of glioma, its size, and the rate of its growth can all affect the symptoms. Common



FIGURE 1. Glioma progression depicted in a detailed process flow, emphasizing key stages and events.

symptoms and indications of glioma comprises headache, nausea, decreased brain activity, memory loss, alterations in personality or temperament, issues of vision, issues with speech [2], [3]. In Figure 1, the method of treating a glioma tumour is shown. In 2007, World Health Organization (WHO) categorized brain tumours according to the type of cell and grade (grades I–IV), adopting histopathological criteria of diffuse gliomas that relate to similarities with suspected cells of origin and anticipated levels of differentiation [4], [5]. Grade I tumours tend to occur in children and are typically benign tumours, indicating that they are usually treatable [6]. Three tumour types are classified as grade II: oligodendrogliomas, astrocytomas, and oligoastrocytomas, which are a combination of both. Adults commonly experience them. All low-grade gliomas have the potential to grow into high-grade tumours in later stages. Anaplastic Astrocytomas, Anaplastic Oligodendroglomas, and Anaplastic Oligoastrocytomas are all examples of grade III tumours. Compared to grade II, they are more assertive and intrusive. According to the WHO classification, grade IV glioma, which is identified as Glioblastoma Multiforme (GBM), is one of the deadliest tumours [6].

Brain tumours classified as gliomas might differ from one another in terms of their genetic and Molecular makeup. Several factors are taken into account when predicting how glioma would behave and how it will progress. Each variable's explanation and potential impact on glioma prediction are Gender, Age at diagnosis, Race, ATRX, PTEN, EGFR, CIC, MUC16, TP53, IDH1, GRIN2A, IDH2, FAT4, FUBP1, BCOR, RB1, CSMD3, NOTCH1, SMARCA4, PIK3CA, NF1, PIK3R1, and PDGFRA [7]. While gender may not have a direct impact on glioma prediction, it can be thought of as a demographic feature that may be associated with other factors. The age of the patient during the diagnosis is a crucial prognostic indicator. In general, younger patients typically experience greater results than older people. For instance, gliomas in paediatric patients could differ in their features and prognoses. The incidence and prognosis of gliomas can vary depending on race. ATRX, PTEN, EGFR, CIC, MUC16, TP53, IDH1, GRIN2A, IDH2, FAT4, FUBP1, BCOR, RB1, CSMD3, NOTCH1, SMARCA4, PIK3CA, NF1, PIK3R1, and PDGFRA are examples of genetic mutations that can occur. These particular genetic changes or mutations may manifest in glioma cells. Each of these changes alters the tumour's Molecular make-up and, consequently, its behaviour. Patients with glioma may have different treatment options and a different prognosis depending on whether these mutations are present or absent. For

instance, better prognoses are linked to IDH1 and IDH2 mutations [8], while poorer prognoses are linked to amplification of EGFR [9] and PTEN loss. TP53 mutations may influence the tumour's virulence [10]. Genetic testing is essential for glioma Molecular profiling in order to identify the tumour subtype and customize treatment. All of these factors may be taken into consideration by glioma prediction models to evaluate the hazards, and possible treatments for specific patients. Machine learning algorithms, for example, can examine a mixture of these elements to forecast how the disease would most likely develop and the best course of treatment. It is imperative to consult with medical professionals who can provide tailored guidance based on these variables and the most recent discoveries about the diagnosis, management, and prognosis of gliomas [11].

Prediction of patient suffering from glioma tumour can be achieved with artificial intelligence and machine learning classifiers. Artificial intelligence (AI) refers to creation of computer systems and algorithms that are capable of performing activities that frequently need human intelligence, like learning from data, reasoning, solving problems, and understanding natural language. Robots and autonomous systems are included, along with the various additional techniques and purposes, including neural networks and machine learning [12]. Algorithms for artificial intelligence (AI) perform complex operations on enormous volumes of data. These activities consist of recognizing text and imaging, remote medical care, precise disease identification, and disease prediction [13]. A subfield of artificial intelligence called machine learning (ML) is concerned with developing algorithms and models that enable computers to process data, draw conclusions, and make predictions without being explicitly programmed [14], [16]. It involves using statistical techniques to help computers become more proficient at a particular task through iterative learning from experience. The healthcare industry can benefit greatly from machine learning since it can analyse vast amounts of patient data to find trends, predict disease outcomes, and help with early diagnosis. In addition, machine learning can be used to streamline administrative procedures, enhance medicine development, and improve treatment regimens, ultimately leading to better patient care and cheaper healthcare costs [17], [18]. As a result of the recognition that classifiers must be utilised appropriately in order to provide transparency, accountability, and ethics, Explainable AI (XAI) was created [15]. Black-box models have new potential because to the explainability element, which also enables healthcare stakeholders the assurance of interpreting deep learning (DL) [19], [20] and machine learning (ML) algorithms [19], [21]. Transparency in predictive analysis is essential for the healthcare sector, and XAI intends to work on improving it [15]. The idea of creating artificial intelligence systems and machine learning models in a way that allows people to understand and interpret its decisions and behaviours is known as explainable artificial intelligence (XAI). XAI aspires to render artificial intelligence accountable and transparent by

outlining the justifications for the decisions that AI systems make [22].

Machine learning algorithms can forecast whether or not a patient has been diagnosed with a glioma tumour using genetic and Molecular makeup markers. By examining a wide range of genetic markers, the algorithms can determine the level of seriousness of the illness of a person and the possibility of complications. This will aid in early diagnosis and detection. It will assist in early treatment planning for patients and prevent subsequent issues, improving the health of the patient. Continuous observation and analysis can also enable early patient intervention for those who are at risk, enhancing overall healthcare and health outcomes. Explainable Artificial Intelligence (XAI) is essential for fostering trust, addressing ethical concerns, ensuring regulatory compliance, debugging models, enhancing user understanding, and promoting collaboration. It provides transparency and interpretability in AI systems, making them more accountable and accessible.

Following is the organization of the remaining content: Related work is illustrated in Section III. Materials and Methods are discussed in the Section IV. The results of the study are discussed in considerable detail in the Section V. Section VI addresses conclusion of the classifiers along with probable applicability.

II. RELATED WORK

To forecast whether the patient is diagnosed with glioma or not, a number of research have already used machine learning approaches. The following research projects have significantly advanced knowledge:

Using multi-modal MR image fusion, Ouerghi et al. [23] examined the function of radiomic feature integration in conjunction with machine learning techniques in the distinction of low-grade gliomas from high-grade gliomas. 80 histologically verified glioma patients from the MICCAI BraTS 2019 dataset i.e., 40 high-grade gliomas and 40 low-grade gliomas were analyzed for this research [23]. Five machine learning algorithms were created and examined using the fused and the recovered data utilizing a tenfold cross-validation plan. As an outcome, the model of random forests, which used 21 characteristics chosen from the raw data, achieved the highest accuracy of 96.5%. Utilizing texture information based on 153 multi-parametric MRI patients, a radiomics approach has been proposed by Tian et al. [24]. For separating grades III from IV and LGGs from HGGs, respectively, SVM models were created utilizing 30 and 28 optimum characteristics. The accuracy of the SVM (support vector machine) algorithm was 96.8% for separating LGGs from the HGGs and 98.1% for separating grade III from grade IV, which was acceptable compared to utilizing single sequence MRI or histogram parameters [24]. A total of 285 cases collected for the Brain Tumour Segmentation 2017 Challenge were examined by Cho et al. [25]. Five prominent characteristics were chosen for the machine learning models using the minimal redundancy maximum

relevance algorithm. The three different classifiers (support vector machines, logistic regression, and random forest) obtained 94% of mean accuracy for training class and 92.13% of maximum accuracy for test class [25]. For training cohorts, they displayed an average AUC of 0.94, whereas for test cohorts, it was 0.9030 (as for logistic regression it is 0.9010, for support vector machine it is 0.8866, and for random forest it is 0.9213). A non-invasive glioma prediction framework is proposed in by Wu et al. [26]. Between 2012 and 2016, experiments were carried out on about 161 cases of glioma from the Henan Provincial People's Hospital. The outcomes showed that the de-redundancy algorithm was widespread and had an accurate grading impact. The 2D segmented tumour was used to calculate 346 radiomics characteristics. A candidate feature was built using mutual information. Then an elastic net was used to carry out the feature selection. The prediction model was developed using linear regression to obtain the necessary sensitivity of 93.57%, specificity of 86.53%, 0.9638 AUC, and 91.30% accuracy. Cao et al. [27] produced a quantitative framework according to the location of tumour and volume of tumour, characteristics employing data from the 229 The Cancer Genome Atlas LGG and GBM patients [27]. Two of the sample approaches were used in the construction and testing of the LASSO regression i.e., least absolute shrinkage and selection operator and nine machine learning models: institution-based and repeat random sampling (with 70% of training set and 30% of validation set) [27]. The best results were obtained via stack modelling and support vector machines (AUC > 0.900, accuracy > 0.790 for validation set derived from institution-based sampling; AUC > 0.930 for average validation set, accuracy > 0.850 for repeat random sampling). The regression model demonstrated the best performance for the LASSO approach (institution-based sample validation set, with AUC 0.909 and model accuracy of 0.830). From 735 photos, Rathore et al. [28] retrieved 2D quantitative imaging characteristics, including conventional, clinical, and textural characteristics. Tenfold cross-validation using the 735 glioma images resulted in a successful verification of the texture features (accuracy: 75.12%, AUC: 0.652) using the SVM algorithm. Table 1. summarizes the related work with a deep and wide review.

The current study is concerned with using XAI methods like Eli5, SHAP, Qlattice and LIME to enhance prediction of glioma, a brain tumour. A recent development in machine learning called Explainable AI (XAI) aims to address the unresolved query of how “black box” artificial intelligence (AI) algorithms determine decisions. In an effort to make decision-making processes and models more understandable and comprehensible, this field conducts research on them.

The findings cited above indicate that prediction has already been done using ML and AI algorithms. The following ways that this article adds to the body of literature:

1. Pearson’s correlation, mutual information and principal component analysis, the feature selection approaches

- were used to identify the most crucial attributes. This study compared different feature selection techniques.
2. A ground-breaking customized “ensemble-stacking” approach was developed and put into use to improve performance using baseline classifiers.
 3. In this unique investigation, four XAI algorithms were applied to the given data to clarify predictions: ELI5, LIME, Qlattice and SHAP.

III. MATERIALS AND METHODS

A. DATASET DESCRIPTION

We used a dataset that has been made available to the public for this study [39]. The UCI Machine Learning Repository has access to the Glioma Grading Clinical and Mutation Features Dataset. Given that gliomas are prevalent primary tumour of brain and are classified as either GBM (Glioblastoma Multiforme) or LGG (Lower-Grade Glioma) based on imaging and histological criteria, the grading procedure heavily relies on the clinical and molecular/mutation aspects. Three clinical characteristics and the twenty most frequently altered genes from TCGA-LGG and TCGA-GBM brain gliomas are taken into consideration in this dataset. The dataset includes the Clinical and Molecular/mutation factors that are used in prediction task to identify patients with specific clinical, molecular, and mutational characteristics as LGG or GBM. The molecular/mutation factors are described as 0 = NOT_MUTATED; 1= MUTATED. There are 889 patients with 23 attributes in this set of patients. The target variable in this dataset is grade (binary classification problem) which stated a patient to have LGG or GBM. Out of 889 patients, 487 suffered with LGG while 352 suffered with GBM. Out of 23 attributes there was 1 numerical attribute and 22 categorical attributes. The attributes had no null values. Table 2 lists the dataset’s attributes.

B. DATASET PREPROCESSING

The processing of dataset turns unprocessed data into forms that are comprehensible and useful. Raw datasets present several issues, including defects, unpredictable behaviour, absence of trends, and unpredictability [40]. Preprocessing is also required for the purpose to address missing values and discrepancies. The dataset was preprocessed, and a few further operations were required to be prepared for employing in deployment.

Balancing the dataset allows for training a model easily by avoiding it from getting biased toward one class. There are two approaches for balancing data: undersampling and oversampling. Despite being simple to construct as well as capable of enhancing model run-time, undersampling has some downsides. The elimination of data points from the original set of data can result in loss of important information. Oversampling in this manner results in false scores from the minority class. So, in this study, the dataset was already appropriately balanced, so there was no need to implement any extra balancing algorithms [41], [42].

Data normalization entails rescaling the attributes to ensure their means and variance are both equal to 0. Standardization aims to preserve the variations in value limitations while reducing every attribute to a comparable scale. We employed the conventional scaler technique for feature scaling. Following the standardization procedure, an outlier has no longer impact on dataset hence, standardization do not have variability restriction.

To allow algorithms to analyze and learn from non-numerical aspects, categorical data must be transformed to numerical format for use in data analysis and machine learning. A key method for characterizing binary vectors of categorical data in machine learning and data analysis is one-hot coding. Every group or label in the dataset appears as a binary vector, with just a single component set to “hot” (set to 1) and all other elements set to “cold” (set to 0). The one-hot encoding method of feature engineering is critical for preparing data for tasks such as classification and regression [43]. For our study, one hot encoding was not performed.

C. FEATURE SELECTION

In this study, Pearson’s Correlation, Principal Component analysis and Mutual information were used to select the best characteristics. These algorithms aided in the extraction of crucial attributes while also reducing the quantity of data.

1) PEARSON’S CORRELATION

Pearson’s correlation coefficient analysis was conducted after an initial assessment of the dataset to see how each attribute influenced the outcome. The coefficient value “r” as well as the output were perfectly associated if the value reached close to “1/1,” while “0” value indicated no association. Positive correlation coefficient value implies that component influenced the outcome positively. If it was unfavorable, the outcome was influenced in the opposite direction. The method for evaluating correlation coefficients is based on an idea that analyzing the degree to which specific variable’s attributes are associated can help to determine the value of attribute collection in a dataset [44], [45]. Few variables correlated positively, while others correlated negatively. Figure 2 depicts the correlation heatmap.

2) MUTUAL INFORMATION (MI)

The Mutual Information Method is one of an effective approach for selecting features [46]. This filtering method requires into consideration the numerical properties of the dataset. Mutual information depends on an entropy, which is the measure of how unpredictable the features are. The qualities were rated according to the relative contribution of each to the desired variable, as shown in Figure 3.

3) PRINCIPAL COMPONENT ANALYSIS (PCA)

Principal component analysis (PCA) is frequently employed in modern data analysis. The purpose of PCA is to find a

TABLE 1. An overview of related work.

Reference	Dataset Used	ML algorithms	Results	Pros	Cons
Emblem et al. [29]	Local dataset consist of 86 glioma patients DSC MRI which further divided into a training dataset of 53 patients and testing dataset of 33 patients	SVM	True positive rate of 0.76 and True negative rate of 0.88	Classification of Low- or High-grade Glioma. Histogram signatures obtained using cerebral blood volume (CBV) values taken from the Tumor ROIs.	Stability of the model for interinstitutional data has not been shown.
Zacharakis EI et al. [30]	Local dataset consist of MRI of 102 cases out of which 24 cases of metastasis, 4 cases of meningioma's, 22 cases of gliomas grade II, 18 cases of gliomas grade III and 34 cases of glioblastomas	SVM	85% (Accuracy) for classifying metastases vs gliomas 88% (Accuracy) for Classifying low grade vs high grade glioma	Classification of Low- or High-grade Glioma	Need for tracing ROIs, which makes the current approach semiautomatic and subject to intra- and interobserver variability.
Lo et al. [31]	TCIA dataset Total =107 (73 LGG, 34 GBM)	logistic regression	88% (Accuracy)	Classify Glioblastomas (HGG) from diffuse lowergrade gliomas (LGG)	Only two-dimensional tumor areas were delineated for feature extraction and subsequent classification.
Subashini et al. [32]	Local dataset consisting of only 200 T2 MRI images of low- and high-grade glioma	SVM, LVQ (Learning vector quantization) and Naive Bayes	88 to 91% (Accuracy)	Classification of Low- or High-grade Glioma. Brain image preprocessing, image segmentation, tumor isolation (ROI), feature extraction, feature selection and classification of selected features to discriminate the grade.	Segmentation of tumor was time consuming and difficult since the tumor boundary need to be preserved without losing shape and grey level information.
Cho et al. [33]	BRATS 2017 dataset consist of MRI sequences of 75 LGG and 210 HGG patients	Logistic Regression (LR), Random Forest (RF), SVM and ensemble of these three classifiers	RF delivers best results with 88.7% (Accuracy), 73.3% (specificity), 94.3% (sensitivity) and 92.13 (AUC)	Classification of Low- or High-grade Glioma. Manual segmentation and set of 468 radiomics features composed of 24 shape-based, 228 histogram-based, and 216 texture-based features extracted from three ROIs.	Independent validation using data from another clinical site is missing. There was a class imbalance between two classes. The ROIs were provided by the database and the reproducibility was not verified. Updated grading of gliomas was unavailable to us and thus we used the information of the traditional grading system.
Chen et al. [34]	Dataset consist of 54 lowgrade and 220 high-grade gliomas MRI sequences taken from the BRATS 2015 challenge	XGBoost	91.27% (Accuracy), 91.27% (Precision), 91.27% (Recall), 90.64% (F1 score)	Classification of Low- or High-grade Glioma. 3D convolutional neural network is used for segmentation.	Most of these studies are based on manually segmented ROIs, which limit the development of radiomics.
Gupta, Rajagopalan and Rao [35]	BRATS 2012 dataset	Naive Bayes classifier	96% (Accuracy), 95% (specificity) and 97% (sensitivity)	Classification of Low- or High-grade Glioma. Texture features extracted with the help of DWT and LBP.	Reduced accuracy might be due to the larger variance in volume-based features within the group of LG and HG patients when real and simulated images are considered together.
Wang et al. [36]	One Local dataset consist of total 146 cases of glioma in which there are 52 cases of grade IV, 45 cases of grade III and 49 cases of grade II images from Shandong Provincial Hospital affiliated to Shandong University	SVM, RF, Gradient boosting decision tree (GBDT) and Neural network (NN)	SVM delivers best results with 94% (Accuracy), 97% (F1 score), 94%(specificity) and 94% (sensitivity)	Glioma into three grades i.e. II, III and IV grade. Whole Slide images (WSI) (Hematoxylin–Eosin (H&E) images).	First, grade I gliomas are not included in our studies. The results of our discrimination of grade III and grade IV are just reasonable preliminary results but leave much room for improvement.
Cao et al. 2020 [37]	Dataset consist of 128 GBMs and 101 LGG patients MRI sequence taken from the Cancer Imaging Archive (TCIA)	Nine classifiers like SVM, Stack modeling, Neural network, Random Forest Naive Bayes k-nearest neighbors	SVM ofers an highest accuracy of 91.7%	Lower grade glioma (grade II and III) or glioblastoma (grade IV). Tumour location and volume-based features, LASSO based feature	This research is based on retrospective data collection, which can inherently have sampling bias. The MNI152 registration procedure in this research is initially designed for healthy individuals in

TABLE 1. (Continued.) An overview of related work.

		AdaBoost etc		selection.	psychological studies; thus, it could result in an inaccurate registration result or other effects in a group of medically ill patients. Since, the anatomical distribution is automatically measured based on the abovementioned registration results, the final tumor location ratio may not perfectly represent the real percentage of tumor in a particular location.
Yang et al. [36]	One local dataset consist of 63 grade IV, 29 grade III and 25 grade II glioma patients MRI sequences	Radial basis function SVM (RBF-SVM)	GLSJM method with RBF SVM delivers highest accuracy of 87.5% and 0.971 (AUC)	Glioma into three grades i.e. II, III and IV grade. Feature selection using SVM-RFE.	Only four commonly used attribute retrieving models were compared in the current study. According to the latest WHO 2016 grading criteria, a future study should be focused on molecular markers, like IDH1/2 and MGMT. Third, this study was a single-center study and the MRI data were obtained using a certain GE scanner. It is unknown whether the technique can be applied independently from GE vendors or not. To test this hypothesis, a multicenter study needs to be done.
Lu et al. [37]	Local dataset consist of total 193 glioma patients MRI (130 Mutant glioma cases and 63 wild glioma cases)	Pyramid dilated convolution ResNet neural network model	80.11%(Accuracy)	Classification of Mutant gliomas or wild gliomas. Preprocessing using Standard deviation. Standardization and normalization. Feature extraction using modified ResNet.	This method only can process 2D volume MRI; second, it needs to select pictures with obvious tumor occupancy and require the assistance of experts to manually label the training set, which is extremely labor-intensive.
Jeong et al. [38]	Local dataset consist of MRI sequences of 25 patients out of which 12 of HG (GBMs) and 13 of LG patients	Random forest	Average (Accuracy) 90%	Classification of Low- or High-grade Glioma.	Only a limited number of patients were available for the study within the inclusion criteria. Only 25 patients had FLAIR and DSC MRI images as well as having either biopsy or tumor resection with histopathological analysis.

highly meaningful foundation for reexpressing a particular set of data. Dimensionality reduction, compression of data, extraction of features, and data visualization are just a few examples of uses. Principal components, which are produced by linearly combining the original variables, are a set of new orthogonal variables produced by PCA [47]. Using Principal Component Analysis (PCA), one can make certain datasets less dimensional. enhances interpretability while retaining most of the information. It accomplishes this by introducing fresh, unrelated covariates. This new variable discovery, or what we refer to as the key components, will lessen the difficulty of solving the eigenvalue/eigenvectors problem [48]. The Principal Component Analysis (PCA) technique aids in determining which set of data most accurately captures the topic under study. People receive several components via the PCA technique, which reduces the dimensionality of a multivariate dataset by condensing the dimensions into a single variable [49] as shown in Figure 4.

4) IMPORTANT FEATURES

Some features that are constant include IDH1, Age at diagnosis, PIK3CA, ATRX, PTEN, CIC, EGFR and TP53. These characteristics were selected to be examined further. Table 3 depicts the list of key features from Pearson's Correlation, Mutual Information and PCA.

D. MACHINE LEARNING TERMINOLOGIES

The steps involved in machine learning are selection and preparation of dataset, model training, model deployment and model's performance assessment. For the purpose of improving the model's performance, iterative testing as well as enhancements to the model are commonly employed. The end result of machine learning is the building of an algorithm that accurately synthesizes to freshly acquired data and addresses the query at hand. To choose the best model, hyperparameter tuning must be effective. Hyperparameter

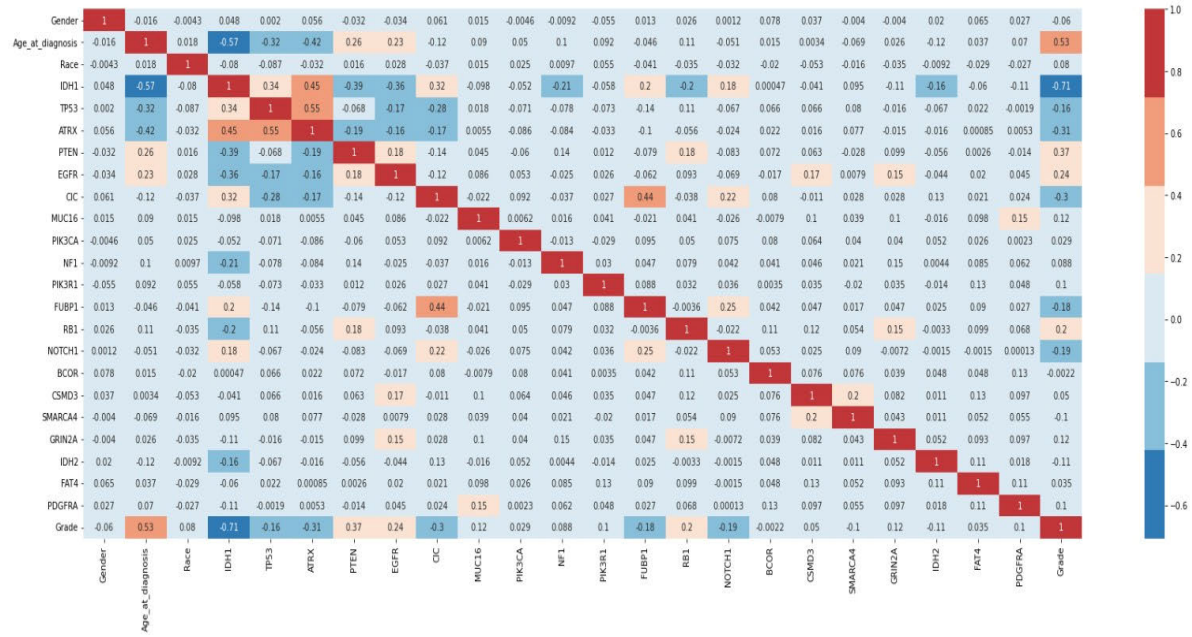


FIGURE 2. Pearson correlation matrix showcasing interrelationships among variables.

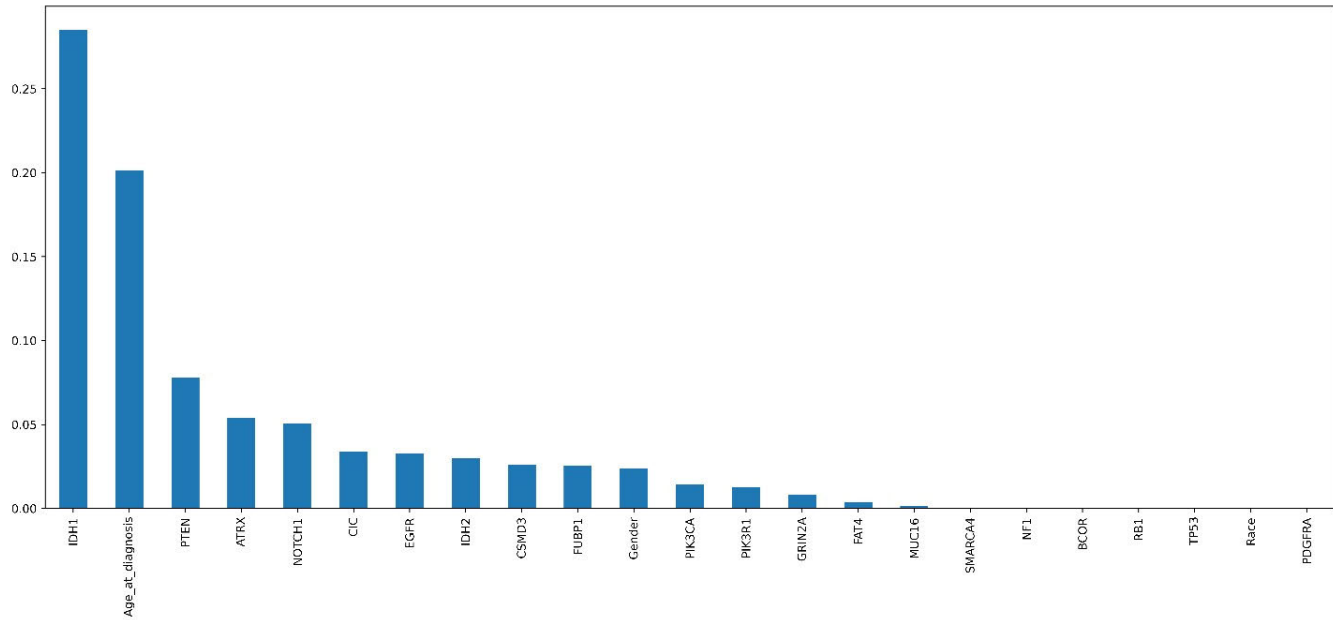


FIGURE 3. The mutual information algorithm ranks traits by their relevance in a concise evaluation.

selection aims to highlight the beneficial outcomes from previous training cycles. Model improvement is possible by modifying the algorithm's parameters [45]. We used the grid search optimization technique in this study which acquire's optimized parameter values. Grid search is a tuning technique that manually examines each value in the predefined hyperparameter space to carry out comprehensive parameter searching. Many machine learning algorithm's performance is influenced by their hyperparameter configurations [50].

Machine learning ensemble models are used in variety of ways, such as bagging, boosting and stacking. By stacking models, we may train several of them to tackle related issues and then integrate the results to create a more powerful model [51]. Making use of this concept, we built three stacks on two distinct levels. Figure 5 illustrates stacking with a graphic demonstration. Random forest, KNN, logistic regression and decision trees made up the initial stack. Tree based models like Xgboost, lightgbm, catboost and adaboost made

TABLE 2. Comprehensive overview detailing the key attributes present in the dataset.

Attribute No.	Attribute Name	Attribute type	Feature	Description
1.	Gender	Quantitative	Clinical	Gender: 0 = male and 1 = female
2.	Age at diagnosis	Numerical-Continuous	Clinical	Age of diagnosis in addition to estimated duration in days
3.	Race	Quantitative	Clinical	Race: 0 = white; 1 = black or African, American; 2 = Asian and 3 = American, Indian or Alaska native)
4.	IDH1	Quantitative	Molecular	Isocitrate dehydrogenase (NADP (+))1 (0 = NOT_MUTATED and 1= MUTATED)
5.	TP53	Quantitative	Molecular	Tumor protein p53
6.	ATRX	Quantitative	Molecular	ATRX chromatin remodeler
7.	PTEN	Quantitative	Molecular	Phosphatase and Tensin homolog
8.	EGFR	Quantitative	Molecular	Epidermal growth factor receptor
9.	CIC	Quantitative	Molecular	Capicua transcriptional repressor
10.	MUC16	Quantitative	Molecular	Mucin 16
11.	PIK3CA	Quantitative	Molecular	Phosphatidylinositol-4,5-bisphosphate 3-kinase catalytic subunit alpha
12.	NF1	Quantitative	Molecular	Neurofibromin 1
13.	PIK3R1	Quantitative	Molecular	Phosphoinositide-3-kinase regulatory subunit 1
14.	FUBP1	Quantitative	Molecular	Far upstream element binding protein 1
15.	RB1	Quantitative	Molecular	RB transcriptional corepressor 1
16.	NOTCH1	Quantitative	Molecular	Notch receptor 1
17.	BCOR	Quantitative	Molecular	BCL6 corepressor
18.	CSMD3	Quantitative	Molecular	CUB and Sushi multiple domains 3
19.	SMARCA4	Quantitative	Molecular	SWI/SNF related, matrix associated, actin dependent regulator of chromatin, subfamily a, member 4
20.	GRIN2A	Quantitative	Molecular	Glutamate ionotropic receptor NMDA type subunit 2A
21.	IDH2	Quantitative	Molecular	Isocitrate dehydrogenase (NADP (+)) 2 (0 = NOT_MUTATED and 1 = MUTATED)
22.	FAT4	Quantitative	Molecular	FAT atypical cadherin 4
23.	PDGFRA	Quantitative	Molecular	Platelet-derived growth factor receptor alpha
24.	Grade	Quantitative	Target	Glioma grade class information (1 = GBM (Glioblastoma Multiforme); 0 = LGG (Lower-Grade Glioma))

up second set of stack. The ultimate stack was created by further ensembling the aforementioned stack.

XAI techniques were applied to interpret the model outputs. The implication of interpretability using XAI models, is the ability to understand and make sense of the decisions or outcomes generated by a model. It provides transparency, ensuring that the inner workings of the model are accessible

and can be explained in a human-understandable manner. The following XAI models were applied to this study:

1. SHAP (SHapley Additive exPlanations): By determining the relative contributions of every feature to resulting estimation and prediction, this model-neutral method assesses the outcome for any machine learning model.

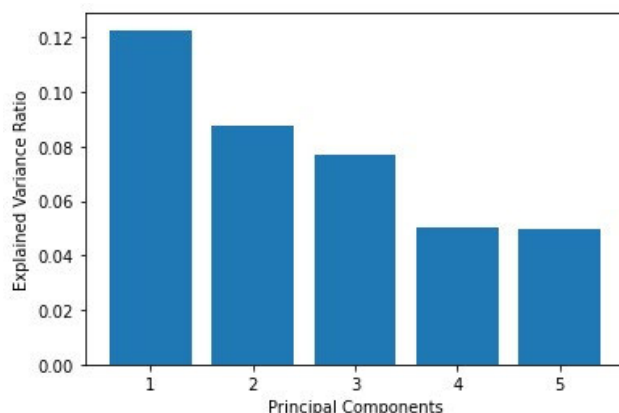


FIGURE 4. Cumulative variation in a dataset visualized through graphical representation.

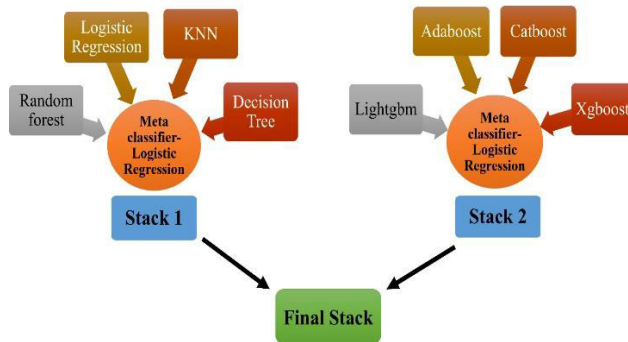


FIGURE 5. Visualization depicting the concept of stacking.

2. LIME (Local Interpretable Model-agnostic Explanations): LIME is an approach that provides interpretations locally of the black-box models through utilizing models that are interpretable and have been trained on subsets of dataset.
3. ELI5 (Explain Like I'm 5): ELI5 is a package in Python which offers more straightforward explanations of the machine learning models with techniques, that includes feature importance, decision trees, and permutation feature importance.
4. Qlattice: This is also a machine learning model visual aid that lets users interactively examine how the model makes decisions by showing how each and every feature/attribute contributes to the final prediction.

An automated machine learning project's entire workflow is achieved using a pipeline of machine learning, which is made up of several connected data processing modules. Preparing the data, selecting the model, selecting features, adjusting hyperparameters, and evaluating are typically involved. By offering a methodical and automated perspective to the whole process, this pipeline has been designed for maximizing efficacy of various machine learning models. The machine learning (ML) pipeline applied in this study is depicted in Figure 6.

TABLE 3. Critical characteristics and key features inherent in the dataset, offering fundamental insights for analysis and interpretation.

Methods Employed	Features
Pearson's Correlation	'Gender', 'Age_at_diagnosis', 'Race', 'IDH1', 'TP53', 'ATRX', 'PTEN', 'EGFR', 'CIC', 'MUC16', 'PIK3CA', 'NF1', 'PIK3R1', 'FUBP1'.
Mutual Information (MI)	'IDH1', 'Age_at_diagnosis', 'PTEN', 'ATRX', 'NOTCH1', 'CIC', 'EGFR', 'IDH2', 'CSMD3', 'FUBP1', 'Gender', 'PIK3CA', 'PIK3R1', 'GRIN2A'.
Principal Component Analysis (PCA)	Top features for Principal Component 1: ['IDH1', 'Age_at_diagnosis', 'ATRX', 'PTEN', 'TP53'] Top features for Principal Component 2: ['CIC', 'FUBP1', 'TP53', 'NOTCH1', 'ATRX'] Top features for Principal Component 3: ['CSMD3', 'FAT4', 'RB1', 'SMARCA4', 'GRIN2A'] Top features for Principal Component 4: ['FAT4', 'IDH2', 'PIK3R1', 'SMARCA4', 'CSMD3'] Top features for Principal Component 5: ['IDH2', 'PIK3R1', 'PIK3CA', 'BCOR', 'NOTCH1']

IV. RESULTS

A. PERFORMANCE METRICS

Our AI models have been evaluated and compared using classification measures like precision, recall, F-1 score, accuracy and AUC score (Area Under the Curve). Our classifiers aim to identify patients with gliomas, a particular type of brain tumour.

1. Accuracy: The accuracy refers to the ability to accurately identify between patients who are having a LGG (Lower-Grade Glioma) or GBM (Glioblastoma Multiforme). To ascertain whether the forecast was accurate, it is necessary to calculate the percentage of true positive as well as true negative outcomes in each of the examined cases.
2. Precision: The proportion of patients who are having a Lower-Grade Glioma or Glioblastoma Multiforme out of all other patients is determined by this statistic. This means that individuals who have been diagnosed with a glioma that was not actually a glioma are also taken into account.
3. Recall: This performance metric is defined as the precise ratio of patients who are having a LGG (Lower-Grade Glioma) to all patients that were impacted. False-negative events are highlighted by this statistic. When the false-negative cases are rare, this metric is quite boosted.
4. F1 score: The combined precision and recall ratings of a model are represented by its evaluation statistic.



FIGURE 6. Essential stages in the machine learning pipeline.

5. AUC: Plotting true positive rate against false positive rate across a range of test parameters is known as ROC curve. It illustrates models' ability to categorize among two distinct binary classes i.e., LGG (Lower-Grade Glioma) or GBM (Glioblastoma Multiforme). AUC is an area under this curve and high values of AUC depict good classifier performance.

B. MODEL EVALUATION

By examining patterns and risk variables, machine learning (ML) algorithms are able to accurately determine an individual's care pathway and present customized guidelines for treatment and prevention. Additionally, by assisting medical professionals in making faster and more accurate diagnoses, they can enhance patient outcomes. The classifiers were

run in the Conda virtual environment, which is integrated with Python. NumPy, scikit, pandas, seaborn, matplotlib, and others were installed as libraries. 8 GB of RAM and “Intel®core (TM) i3” CPU was employed in training of the models. An operating system of Windows 64-bit was used for this study’s execution.

Each model was trained using a training-to-testing ratio of 80:20. Table 4 summarizes the findings for Pearson’s correlation, Principal Component Analysis and Mutual Information from several kinds of Deep learning (DL) and Machine learning (ML) models. The results showed that Xgboost performed best with precision of 0.82, F1-score of 0.88, accuracy of 0.88, recall of 0.94, and AUC of 0.92. While the results of Final Stack model were 0.79, 0.82, 0.82, 0.85, and 0.90 for precision, accuracy, recall, F1-score and AUC, respectively.

TABLE 4. Summary of outcomes derived from the machine learning models employed in this research when applied to the test dataset.

Model	Accuracy	AUC	Precision	Recall	F1-Score	Hamming Loss	Log Loss	Jaccard Score	MCC
Random Forest	0.85	0.91	0.81	0.89	0.85	0.148	5.139	0.736	0.705
Logistic Regression	0.85	0.90	0.80	0.90	0.85	0.154	5.345	0.731	0.696
Decision Tree	0.87	0.88	0.82	0.92	0.87	0.131	4.523	0.768	0.744
KNN	0.79	0.87	0.82	0.70	0.75	0.214	7.401	0.604	0.572
SVM (linear)	0.86	0.89	0.80	0.94	0.86	0.142	4.934	0.755	0.726
SVM (Sigmoid)	0.34	0.76	0.20	0.14	0.17	0.660	22.820	0.090	-0.367
Stack 1 (RF, LR, DT, KNN)	0.81	0.89	0.79	0.81	0.80	0.190	6.578	0.666	0.618
Adaboost	0.86	0.90	0.80	0.94	0.87	0.136	4.728	0.762	0.736
CatBoost	0.86	0.91	0.80	0.94	0.86	0.142	4.934	0.755	0.726
LGBM	0.86	0.89	0.80	0.94	0.86	0.142	4.934	0.755	0.726
XgBoost	0.88	0.92	0.82	0.94	0.88	0.125	4.317	0.778	0.757
Stack 2	0.86	0.92	0.82	0.90	0.86	0.142	4.934	0.747	0.718
Final Stack	0.82	0.90	0.79	0.85	0.82	0.178	6.167	0.690	0.644
Ridge Classifier	0.86								
C4.5 Algorithm	0.81								
CART (Classification and Regression Trees)	0.82								
CNN	0.84	0.88	0.80	0.89	0.84	0.160	5.550	0.721	0.683
ANN	0.84	0.88	0.80	0.8	0.84	0.160	5.550	0.721	0.683

TABLE 5. Compilation of hyperparameters utilized in the Grid Search process.

Sr. no.	Classifier	Hyperparameters	Sr. no.	Classifier	Hyperparameters
1.	Random Forest	{bootstrap: True, max_depth: 100, max_features: 2, min_samples_leaf: 4, min_samples_split: 12 and n_estimators: 100}	10.	LGBM	{lambda_11: 0, lambda_12: 0, min_data_in_leaf: 100, num_leaves: 31, reg_alpha: 0.1}
2.	Logistic Regression	{C: 10, penalty: l2}	11.	XgBoost	{colsample_bytree: 0.4, gamma: 0.0, learning_rate: 0.05, max_depth: 3, min_child_weight: 1}
3.	Decision Tree	{criterion: entropy, max_depth: 30, max_features: auto, min_samples_leaf: 5, min_samples_split: 30, splitter: random}	12.	Stack 2	{average_probas: False, max_iter: 9000, use_probas: True, meta_classifier: logistic regression}
4.	KNN	{n_neighbors: 4}	13.	Final Stack	{max_iter: 9000, average_probas: False, meta_classifier: logistic regression, use_probas: True}
5.	SVM (linear)	(kernel='linear', Probability=True)	14.	Ridge Classifier	-
6.	SVM (Sigmoid)	(kernel='sigmoid', Probability=True)	15.	C4.5 Algorithm	-
7.	Stack 1 (RF, LR, DT, KNN)	{average_probas: False, meta_classifier: logistic regression, use_probas: True}	16.	CART (Classification and Regression Trees)	-
8.	Adaboost	{learning_rate: 0.01, n_estimators: 1000}	17.	CNN	(optimizer='adam', loss='binary_crossentropy', Metrics='accuracy')
9.	CatBoost	{border_count: 32, depth: 1, iterations: 250, l2_leaf_reg: 1, learning_rate: 0.03}	18.	ANN	(optimizer='adam', loss='binary_crossentropy', Metrics='accuracy', learning_rate=0.0001)

Log loss of 6.167, hamming loss of 0.178, jaccard score of 0.690, and Mathew's correlation coefficient (MCC) of 0.644 are the related loss metrics for Final Stack. Table 3 displays summary of these test results.

Using Grid Search approach and 5-fold cross-validation, hyperparameter adjustment was applied to all algorithms in order to prevent overfitting. The models' selected hyperparameters are listed in Table 5.

The AUCs for the final stack model is represented in Figure 7. For test size = 0.2 and balanced data, final stack model received AUC value of 90%. The precision-recall

(PR) curve and confusion matrix of the final stack model is demonstrated in Figure 7 with a precision of 79%. This study used heterogenous classifiers along with feature selection techniques to enhance performance. To help doctors in predicting whether the patient is diagnosed with glioma tumour i.e., Lower-Grade Glioma or Glioblastoma Multiforme, these models could be deployed in the hospitals.

Major objective of deep learning (branch of machine learning) is to train the artificial neural networks for learning and prediction from data. Its capacity to automatically identify and depict intricate patterns in data has led to its

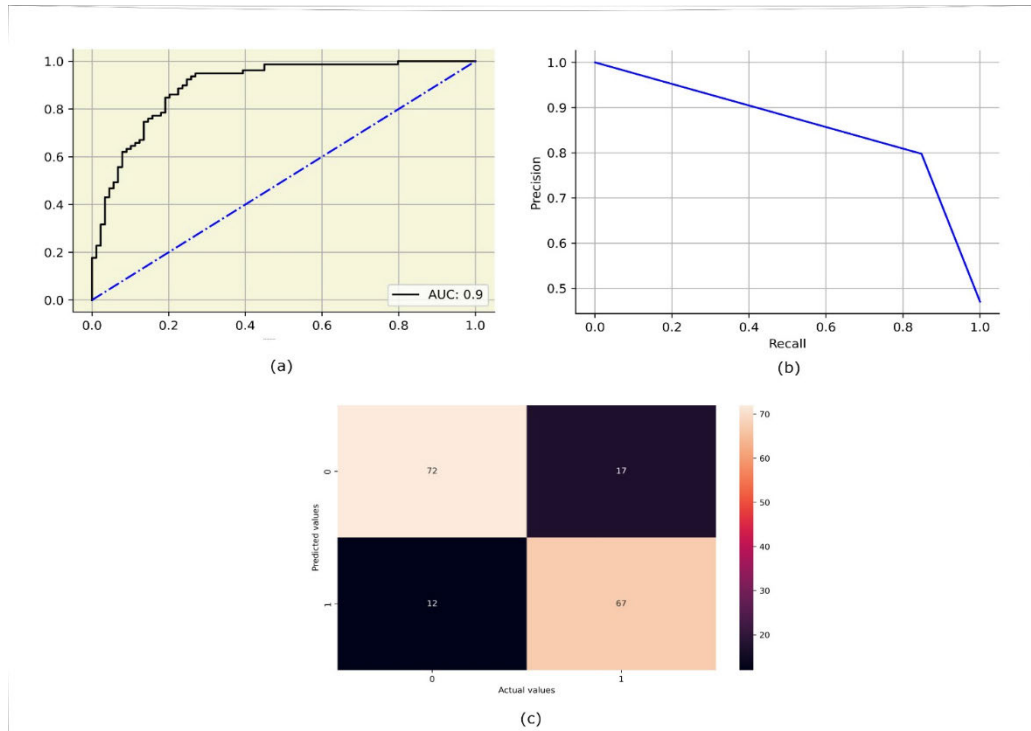


FIGURE 7. a) AUC curve, b) PR curve, and c) Confusion matrix for the final stack model.

enormous rise in popularity. This makes it ideal for a variety of applications, including natural language processing, autonomous systems, image and speech recognition, and more. The ability of deep learning models, especially deep neural networks with numerous hidden layers, to automatically extract hierarchical features from unprocessed data enables them to carry out tasks that were once believed to be beyond the scope of traditional machine learning techniques. Deep learning continues to expand our knowledge of artificial intelligence and has revolutionized a number of areas, including healthcare, banking, and self-driving automobiles [52].

Artificial Neural Networks (ANNs) are computer processing devices which heavily borrow from how the human brain operates. An enormous number of interconnected computational nodes (neurons) form the fundamental building block of artificial neural networks (ANNs). These distributed neurons work together to optimize the outcome and learn from the input. [53]. The input layer receives the data, which is subsequently distributed to the hidden layers after it's loaded as a multidimensional vector. The hidden layers perform the learning process, using the preceding layer's decisions to assess whether a stochastic modification will eventually enhance or damage the output. The term "deep learning" refers to systems that have multiple hidden layers stacked on top of each other [53]. In our study, we have employed ANN architecture to predict whether the patient is suffering Lower-Grade Glioma (LGG) or Glioblastoma Multiforme (GBM) and this model has performed with 84% accuracy, 88% AUC

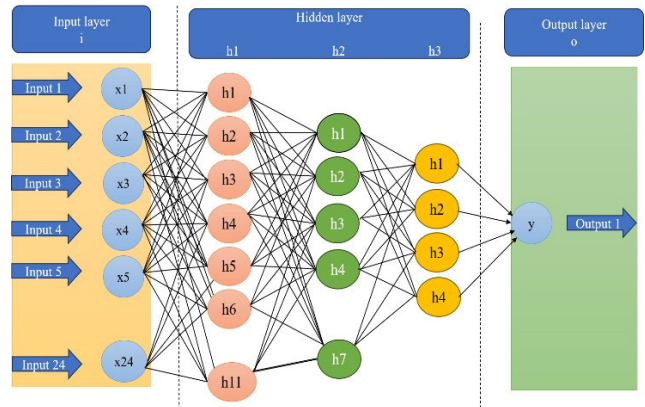


FIGURE 8. Configurational layout defining the architecture of the artificial neural network (ANN).

and 80% precision. An ANN architecture for Glioma classification is illustrated in Figure 8.

ReLU served as an input and hidden layers' activation function, while for output layer, sigmoid served as an activation function. As seen in Figure 9, the accuracy of the test and training sets is satisfactory for ANN architecture for 30 epochs. Figure 10 for the same model architecture and for 30 epochs illustrates the training and validation losses acquired for additional analysis, with a drop in the loss throughout training indicating good convergence.

Similar to traditional artificial neural networks (ANNs), convolutional neural networks are composed of neurons

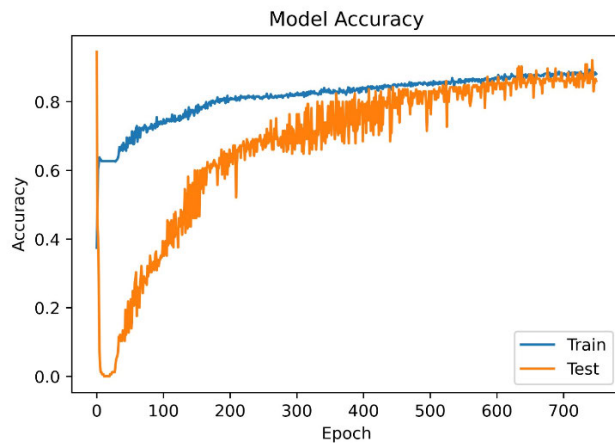


FIGURE 9. Accuracy curve depicting the performance of the artificial neural network (ANN).

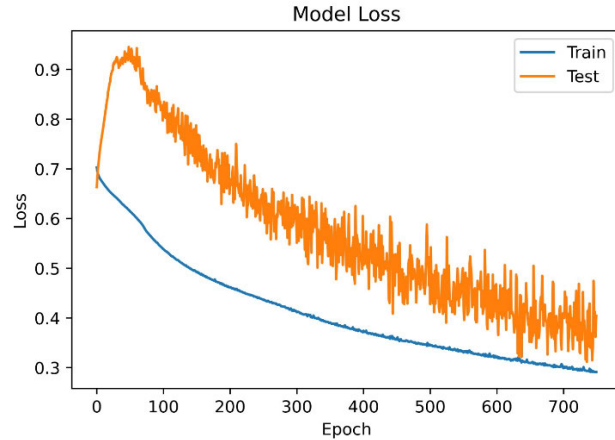


FIGURE 10. Loss curve illustrating the performance of the artificial neural network (ANN).

which can learn to optimize by themselves. The fundamental component of innumerable artificial neural networks (ANNs) is still a single neuron that receives an input and then executes action (like scalar product following non-linear function) [53].

The class score that is generated as the ultimate output will still be represented by the network using single perceptual scoring function (weight) from the initial picture vectors that are input. The last layer of the architecture, which will have loss functions linked to the classes, complies with all the usual rules designed for an ordinary ANNs [53].

The primary application of CNNs is in pattern detection inside images, which is sole discernible distinction among them and ANNs. This further minimizes the number of parameters required to initialize the model and allows us to incorporate attributes unique to individual images into design, thereby improving network's suitability for image-focused applications. CNN's primary benefit over its predecessors is that it can identify important traits automatically without

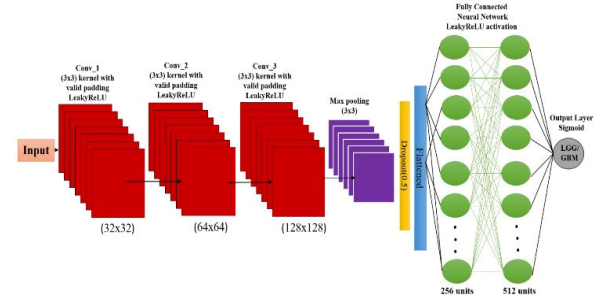


FIGURE 11. Architectural configuration delineating the structure of the Convolutional Neural Network (CNN).

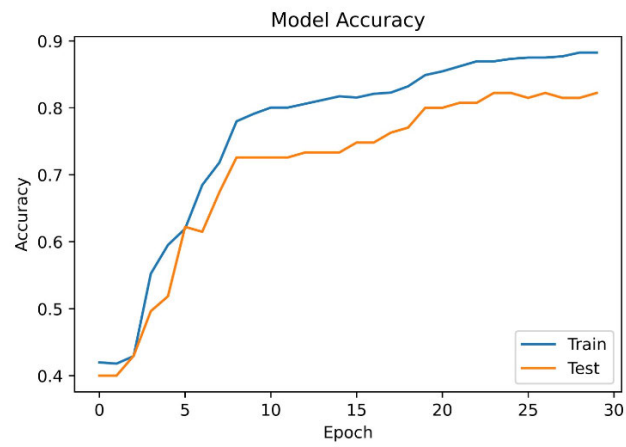


FIGURE 12. Accuracy curve illustrating the performance of the convolutional neural network (CNN).

human oversight, making it the most widely used [54]. Convolutional neural networks are made up of several building pieces, including fully connected, pooling, and convolution layers. They use a backpropagation algorithm to autonomously and adaptively learn the spatial hierarchies of information [55]. Convolutional neural networks are a kind of feedforward neural network which are capable of extracting features from data that has convolution patterns. Unlike traditional feature extraction methods, CNN does not require human feature extraction. CNN's architecture is influenced by how people see things. An artificial neuron is analogous to a biological neuron; CNN kernels are diverse sensors that can react to varied stimuli; activation functions mimic the process by which neural electric signals that surpass a specific threshold are passed on to the subsequent neuron. The creation of loss functions and optimizers allowed the CNN system as a whole to learn what is expected [56].

In our study, we have employed ANN architecture to predict whether the patient is suffering from Lower-Grade Glioma (LGG) or Glioblastoma Multiforme (GBM) and this model has performed with 84% accuracy, 88% AUC and 80% precision. The CNN architecture for Glioma classification is illustrated in Figure 11.

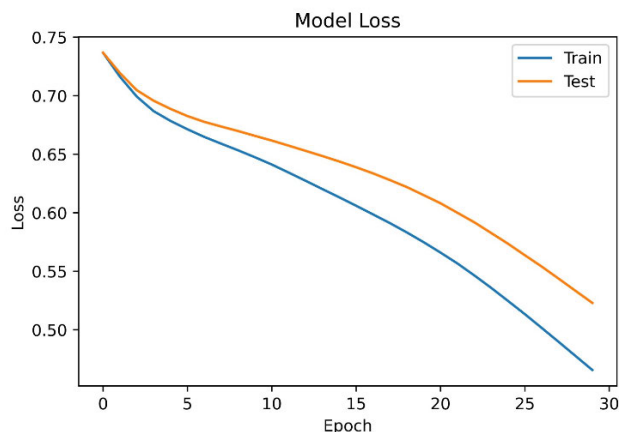


FIGURE 13. Loss curve depicting the performance of the convolutional neural network (CNN).

LeakyReLU was the activation function employed in the convolution layers as well as in the dense layers, whereas sigmoid was used in the output layer. As seen in Figure 12, the accuracy of the test and training sets is satisfactory for CNN architecture for 30 epochs. Figure 13, for the same model architecture and epochs illustrates the training and validation losses acquired for additional analysis, with a drop in the loss throughout training indicating good convergence.

The results obtained from the various models are visually depicted in form of a bar graph in the Figure 14. The dataset is shuffled in the beginning and the data is divided in ratio 80:20 (train: test). This train data is also validated on all the models and results obtained, depict that the models overcome issue of overfitting. Table 6 summarizes the result on training data.

C. EXPLAINABLE ARTIFICIAL INTELLIGENCE (XAI)

Within the healthcare industry, XAI is still in its infancy, despite its promise to enhance the use of AI. Interpretability serves as a guiding principle in the responsible deployment of AI, ensuring that complex models can be understood and scrutinized. It not only reinforces trust and compliance but also empowers users to harness the benefits of advanced technologies while remaining vigilant to potential biases and ethical considerations. The right models can be (semi-)automatically found, their criteria and justifications optimized, partners included, analytics incorporated, a level of safety and accountability recommended, and strategies for integrating them with clinical workflow recommended [57]. Four XAI models are used in this study: QLattice, Eli5, SHAP and LIME. With the use of the feature importance methodologies discussed above, we can better comprehend the relevance of certain qualities. For interpretation, the final stacking model was used [58].

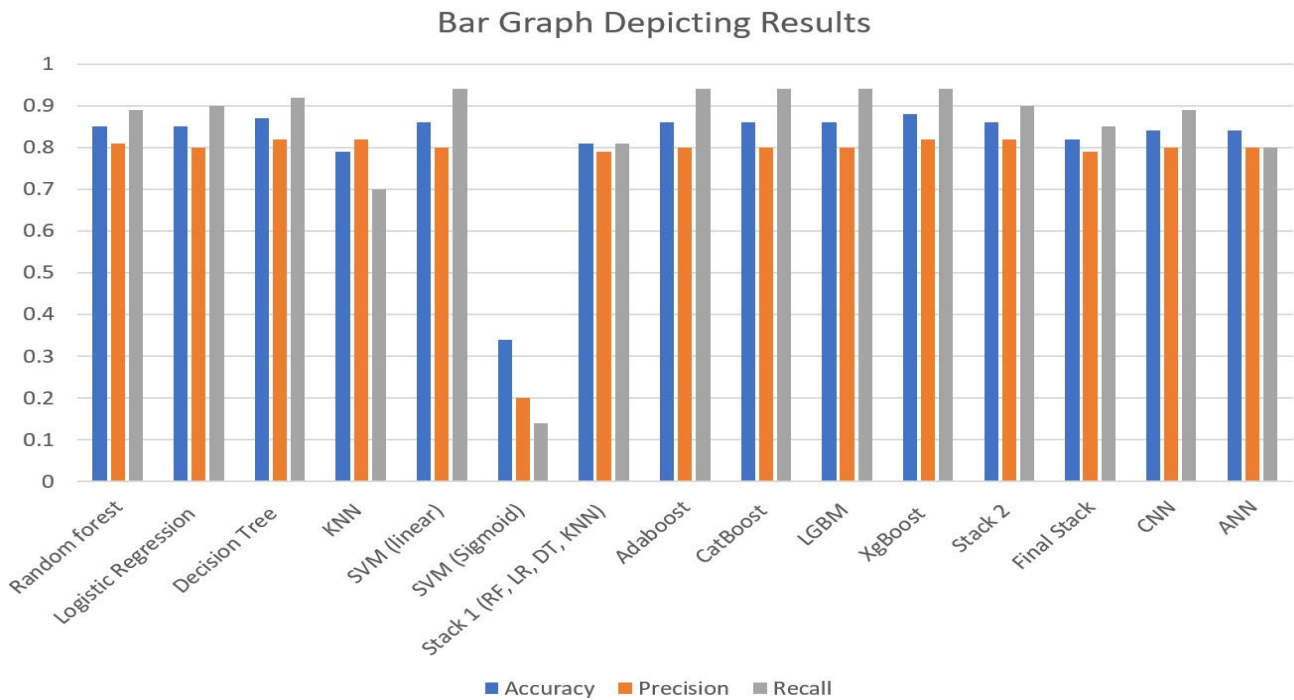
The significance of every feature to machine learning model's prediction are considered by SHAP model in order

to interpret model's output. [59]. By applying principles from game theory, it calculates an insight of each attribute to the model's output and offers comprehensible and straightforward explanations. This procedure is used to assess the prediction's accuracy [60]. Figure 15 shows the beeswarm plot and Bar Chart produced by SHAP analysis for local interpretation. According to the figure, the primary risk factors for glioma tumour in a patient are IDH1, Age at diagnosis, ATRX, CIC, PTEN, EGFR, IDH2, RB1, TP53, MUC16, NOTCH1 and FUBP1.

The machine learning model's predictions are explained via the LIME technique, which creates a locally relevant model centered on the anticipated spot [60]. By selecting the portion of the initial properties that are most important in predicting and building basic model to explain the correlation among all the characteristics and model's yield, it produces interpretations that are understandable locally. Patients with gliomas, categorized as either Glioblastoma Multiforme (GBM) or Lower-Grade Glioma (LGG), are seen in Figure 16. Drawing conclusions from this figure, it can be inferred that green color in bar chart demonstrates attributes and features, critical in determining patient's likelihood of having GBM (Glioblastoma Multiforme), while the red colour indicated the factors that were crucial for predicting that the patient has LGG (Lower-Grade Glioma).

Eli5 is an another XAI technique for interpreting and evaluating the model predictions. It functions as python toolkit for visualizing and debugging predictions using standard API. It facilitates investigators understanding of black-box models and also provides functionality for multiple platforms [61]. Figure 17 depicts how many factors impacted the capacity of various activities to forecast whether patient is diagnosed with glioma brain tumour. The chart demonstrates that IDH1, Age at diagnosis, Race, PIK3CA, BCOR, CIC, PDGFRA and EGFR are the most important features in predicting glioma.

QLattice is a quantum mechanics-inspired machine learning platform that uses a probabilistic Graphical Model to find complex connections and patterns in data [62]. Several thousand of potential models are examined by QLattice before selecting the model which most effectively addresses the present issue. The programmer must initially set up few variables, including labels, input properties, and other variables. These variables are referred as registers. Once the registers are defined, more models can be derived from this particular XAI technique. Model collection is referred as "QGraphs" and these graphs are made up of nodes and edges. Every node includes an activation function, while every edge has the weight assigned to it. The "QGraph" is run using the features to generate important knowledge. The QLattice module in Python is implemented using the "Feyn" package. The QGraph is displayed in Figure 18, and Equation (a) give an explanation of the model's transfer function as well as information about mutual information, Pearson's correlation and Principal component analysis. The data indicates that the

**FIGURE 14.** Bar graph Depicting various models results.**TABLE 6.** Summary of outcomes derived from the machine learning models employed in this research when applied to the training dataset.

Model	Accuracy	AUC	Precision	Recall	F1-Score	Hamming Loss	Log Loss	Jaccard Score	MCC
Random Forest	0.87	0.94	0.81	0.90	0.85	0.127	4.375	0.743	0.745
Logistic Regression	0.88	0.94	0.82	0.92	0.87	0.116	4.015	0.762	0.767
Decision Tree	0.76	0.84	0.64	0.94	0.76	0.243	8.390	0.611	0.572
KNN	0.87	0.95	0.91	0.75	0.82	0.131	4.529	0.700	0.728
SVM (linear)	0.88	0.93	0.80	0.93	0.86	0.123	4.272	0.753	0.756
SVM (Sigmoid)	0.36	0.76	0.19	0.18	0.19	0.636	21.980	0.103	-0.335
Stack 1 (RF, LR, DT, KNN)	1.00	1.00	1.00	1.00	1.00	0.000	0.000	1.000	1.000
Adaboost	0.88	0.94	0.80	0.93	0.86	0.120	4.170	0.758	0.762
CatBoost	0.87	0.93	0.80	0.93	0.86	0.125	4.324	0.750	0.753
LGBM	0.86	0.94	0.80	0.89	0.84	0.137	4.735	0.725	0.724
XgBoost	0.88	0.95	0.81	0.92	0.86	0.117	4.066	0.760	0.765
Stack 2	0.88	0.95	0.82	0.90	0.86	0.122	4.221	0.750	0.754
Final Stack	1.00	1.00	1.00	1.00	1.00	0.000	0.000	1.000	1.000
Ridge Classifier	0.87								
C4.5 Algorithm	1.0								
CART (Classification and Regression Trees)	1.0								
Perceptron Algorithm	0.68								
CNN	0.92	0.97	0.86	0.96	0.90	0.083	2.882	0.823	0.834
ANN	0.92	0.97	0.86	0.96	0.90	0.083	2.882	0.823	0.834

most significant factors for glioma prediction are IDH1, Age at diagnosis and IDH2. The ‘add’ function is also used to comprehend the results.

Based on the previously discussed XAI approaches, the beeswarm plot shows how all the qualities work together

to predict glioma in relation to SHAP. The force plot only shows the most important characteristics that enhance glioma prediction [63], [64]. SHAP can be interpreted locally as well as globally. In comparison to previous XAI techniques, a variety of visualization plots are offered to help comprehend

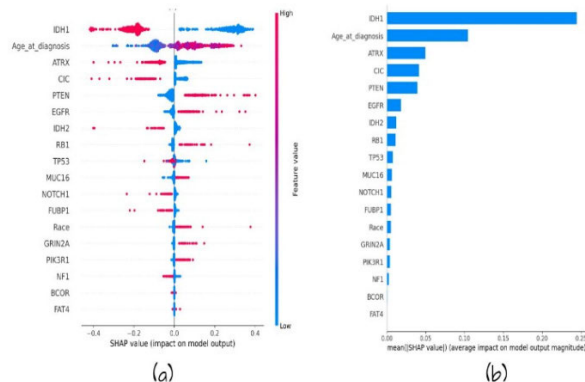


FIGURE 15. Interpretation of SHAP values: (a) Beeswarm plot, (b) Bar Chart.

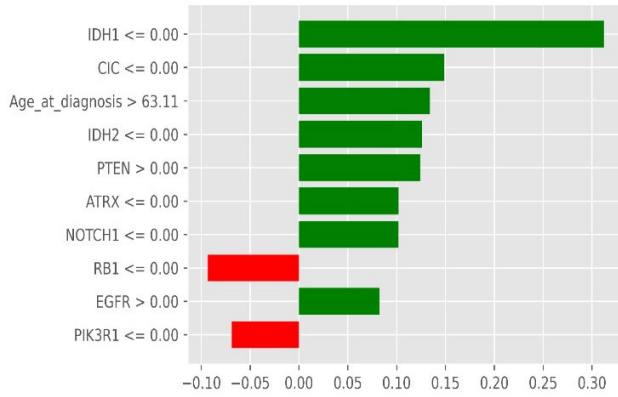


FIGURE 16. Interpretation of LIME (Local interpretable model-agnostic explanations) in predicting patients with glioma tumors.

y=0.0 (probability 1.000) top features

Contribution?	Feature	Value
+0.598	<BIAS>	1.000
+0.360	IDH1	1.000
+0.024	Age_at_diagnosis	44.250
+0.010	Race	0.000
+0.010	PIK3CA	0.000
+0.005	BCOR	0.000
+0.005	CIC	0.000
+0.003	PDGFRA	0.000
+0.003	EGFR	0.000
-0.017	TP53	1.000

FIGURE 17. Explaining model predictions like you're 5 (ELI5): Simplifying complex model outcomes for easy understanding.

an importance of each feature. Each attribute's contribution in predicting glioma can be seen in LIME.

We have created visualizations for those who have suffered with LGG (Low Grade Glioma) an GBM (Glioblastoma Multiforme) [65], [66]. The weights of the qualities are revealed in LIME. However, in this case, our understanding is local rather than global. This implies that individual

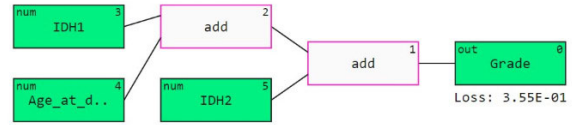


FIGURE 18. Model predictions elucidated through QGraph and transfer function for a comprehensive understanding.

patient forecasts are the only ones that can be investigated in greater detail in LIME. The claim is supported by Qlattice's demonstration of the key factors that cause glioma and by a transfer equation [67], [68]. With the use of the popular quantum computing approach, Qlattice, the model is trained to recognise predictions. However, in comparison with other methods, it requires a large amount of processing time and resources. Qlattice instructs the model to recognise predictions by utilising the popular quantum computing technology. But when compared to other approaches, it requires a lot of processing effort and resources. The relative significance of each characteristic in predicting gliomas is shown by Eli5 [69]. Eli5 is an incredibly effective method for tree-based models, including random forests and decision trees. However, as of right now, deep learning classifiers and other baseline models, such as Eli5, are not supported.

V. DISCUSSION

This study employed machine learning to evaluate a patient's risk for either an LGG or a GBM. The dataset contained 889 patients in total. Pearson's correlation, Principal component analysis and Mutual information were employed in feature selection process. The Machine learning models that were used for prediction included Random Forest, Decision Tree, KNN, Logistic Regression, SVM (Linear, Sigmoid), Stack 1 (RF, LR, DT, KNN), AdaBoost, CatBoost, LGBM, XgBoost, Stack 2, and Final Stack. To enhance our comprehension of the outcomes, four XAI procedures were employed, and a comparison of the methods was conducted. As a preliminary decision support system, glioma tumour can be predicted using the ML model. The Final Stack model was used for prediction since it performed better than any other model. In order to improve our understanding of the results, four XAI methodologies—SHAP, Eli5, LIME and Qlattice were used, and approaches were contrasted.

Machine learning (ML) models that evaluate medical imaging data, including MRI scans, are used to predict glioma tumours, that includes low-grade gliomas and high-grade glioblastomas i.e., Glioblastoma Multiforme, by identifying the tumour type and stage based on features including size, shape, and location. To improve forecasts, these models additionally take into account patient characteristics including age, gender, family history, pre-existing diseases, and genetic data. Tumour progression and possible transition into GBM are assessed by taking into account treatment history and responsiveness to medicines. Predicting the entire impact

of glioma tumours requires an understanding of patient outcomes, including survival rates and quality of life. ML models enable medical personnel to make informed treatment decisions for patients with gliomas by combining information from many sources.

Glioma is the most ordinary primary cerebral tumour, affecting about 7 out of 100,000 people globally annually [70]. Glioblastoma (GBM) is prevalent and malignant form of glioma; despite great efforts and significant progress over the past few decades in understanding the root causes of glioma development, there is still no remedy for GBM, and an average duration of patients' survival with this particular diagnosis is till 12 to 15 months [70]. The writers of the Upsala Journal of Medical Sciences, one of the oldest medical publications in Sweden, have offered a medical perspective on the attributes leading to the prediction of glioma tumours, as XAI models have interpreted the anticipated results. Large-scale genomic analyses of glioblastoma (in humans) have revealed many genes which are mutated. These analyses indicate that the three main signaling connections are disrupted in the majority of tumors: p53 pathway, which is primarily regulated by p53 and p14; receptor tyrosine kinase (RTK)/RAS/PI3K pathway, which is primarily regulated by EGFR amplification, PDGFRA overexpression or amplification, and PTEN inactivation [70]. Authors of The Chinese Medical Journal have provided a medical viewpoint on the characteristics that contribute to the likelihood of glioma tumours [71]. Genetic alterations like BRAFV600E mutation, FGFR1 alteration, MYB or MYBL1 rearrangement are often observed in only low-grade gliomas, whereas high grade gliomas include diffuse hemispheric glioma with H3G34-mutant, midline glioma with H3K27 altered, TP53 and ATRX mutations, and H3G34-mutant glioma [72]. The New England Journal of Medicine (NEJM) reports that gliomas have changes to a number of genes, such as PTEN, TP53, EGFR and CDKN2A. While a tumour progresses towards a high grade, these changes typically take place in a specific order. Though EGFR amplification and PTEN loss or mutation are suggestive of higher-grade tumors, the TP53 mutation appears to happen quite early in the formation of an astrocytoma [73], [74].

Several studies have employed different kinds of machine learning and deep learning models to enhance prediction and forecasting of glioma tumour. A range of machine learning techniques were employed by Niu et al. [75] in his study, to uncover the molecular pathways behind gliomas using machine learning techniques in conjunction with protein-protein interaction networks. Consequently, there are 19 genes separating grade I and grade II, 21 genes separating grade II and grade III, and 20 genes separating grade III and grade IV. The glioma phases were then predicted using five machine learning techniques based on the chosen critical genes. The grade II–III prediction framework was then developed using a supplementary naive bayes classifier that was 72.8% accurate after comparison. Furthermore, random

forest was used in the construction of the grade I–II and the grade III–IV prediction model, which yielded accuracy rates of 97.1% and 83.2%, respectively. Sun et al. [76] aimed to examine the glioma grading estimation efficacy of commonly used radiomics feature selection and categorization methods. Using MRI data, quantitative radiomics characteristics were derived from the tumor areas of 210 patients with Glioblastoma Multiforme and 75 patients with Low-grade glioma. Next, two different test modes, 15 feature selection and 15 classification algorithms were examined for their diagnostic performance using ten-fold cross-validation and percentage split. To further optimize the prediction, roles of tumour sub-region, MRI modality, feature type, and quantity of selected characteristics were compared. According to the results, the best performance in differentiating between LGG and GBM was obtained by integrating the multilayer perceptron classifier with the linear support vector machine feature selection method. This was observed in both percentage split (0.953, AUC:0.981) and ten-fold cross validation (0.944, AUC:0.986). Bhatele et al. [77] provided an overview of the most advanced machine learning-based methods for classifying gliomas. This suggested method was based on the application of a hybrid feature extraction approach and hybrid ensemble learning model, which uses the Central pixel Neighbourhood Binary pattern, Discrete wavelet Decomposition and Gray level run length matrix techniques to classify glioma, into two grades based on fused MRI sequences: Low grade Glioma and High-grade Glioma [77]. This hybrid ensemble learning model, called the Improved eXtreme Gradient Boosting model, was utilized in this work. Two popular global datasets are used to evaluate the proposed method: BRATS 2013 and BRATS 2015, which include a range of MRI fusion combinations, and a well-balanced local dataset comprising of MRI images of low-grade and high-grade glioma from different Madhya Pradesh, India MRI centers. Utilizing the suggested method, the Enhanced eXtreme Gradient Boosting ensemble model yielded an optimal accuracy of more than 90% on the local dataset with resultant fusion of T1C + T2 + Fair MRI sequences. Sudre et al. [78] conducted a study to assess diagnostic value of a dynamic susceptibility contrast MRI paradigm in the classification of treatment-naïve gliomas into grades II–IV and across isocitrate dehydrogenase (IDH) mutation condition in a multicenter patient group. Retrospective identification was done on 333 individuals from 6 tertiary centers who were both molecularly and histologically diagnosed with primary glioma tumour (IDH-mutant = 151 or IDH-wildtype = 182). Using the collected characteristics, a random-forest technique was used to estimate and predict grades or mutation condition. Over 53% of gliomas were correctly categorized when the gliomas were graded, and 87% of the cases had a grade classification. Table 7. displays a deeper description on the important markers used to predict glioma and Table 8. displays comparison of our suggested methodology with the models that are currently in use.

TABLE 7. An overview of markers used to predict glioma.

Sr No.	Markers	Variations	Description
1.	IDH1	Increase in Glioblastoma Multiforme	IDH1, or Isocitrate Dehydrogenase 1, is a gene that encodes a metabolic enzyme. Mutations in IDH1 are commonly found in gliomas, influencing the tumor's molecular profile and prognosis.
2.	TP53	Increase in Low grade glioma	TP53, or Tumor Protein p53, is a critical gene in regulating cell cycle and preventing tumor formation. TP53 mutations are frequently observed in gliomas, impacting cellular functions and contributing to the development and progression of these brain tumors.
3.	ATRX	Increase in Glioblastoma Multiforme	ATRX, or Alpha Thalassemia/Mental Retardation Syndrome X-Linked, is a gene relevant to gliomas, playing a role in chromatin remodeling. Mutations in ATRX are associated with specific subtypes of gliomas, impacting the tumor's molecular characteristics and clinical behavior.
4.	PTEN	Increase in Glioblastoma Multiforme	PTEN, or Phosphatase and Tensin Homolog, is a tumor suppressor gene. In gliomas, alterations in PTEN are common and can lead to dysregulation of cell growth and survival, contributing to the development of these brain tumors.
5.	EGFR	Increase in Glioblastoma Multiforme	EGFR, or Epidermal Growth Factor Receptor, is a gene encoding a cell surface receptor. Amplifications and mutations in EGFR are frequently observed in gliomas, influencing cell proliferation and contributing to the pathogenesis of these brain tumors.
6.	CIC	Increase in Glioblastoma Multiforme	CIC, or Capicua Transcriptional Repressor, is a gene involved in transcriptional regulation. Mutations in CIC are implicated in certain gliomas, impacting cellular processes and contributing to the molecular heterogeneity of these brain tumors.
7.	MUC16	Decrease in Glioblastoma Multiforme	MUC16, or Mucin 16, is a gene that encodes a cell surface glycoprotein. In cancer, including certain types of gliomas, overexpression or mutations in MUC16 may contribute to altered cellular functions and tumor progression.
8.	PIK3CA	Increase in Glioblastoma Multiforme	PIK3CA, or Phosphatidylinositol-4,5-Bisphosphate 3-Kinase Catalytic Subunit Alpha, is a gene encoding a subunit of PI3K. Mutations in PIK3CA are implicated in gliomas, affecting the PI3K signaling pathway and contributing to aberrant cell growth and survival in these brain tumors.
9.	NF1	Decrease in Glioblastoma Multiforme	NF1, or Neurofibromin 1, is a tumor suppressor gene. Mutations in NF1 are associated with neurofibromatosis type 1 and are also found in some gliomas, influencing cell growth and contributing to tumor development.
10.	PIK3R1	Increase in Low grade glioma	PIK3R1, or Phosphoinositide-3-Kinase Regulatory Subunit 1, is a gene encoding a regulatory subunit of PI3K. Mutations in PIK3R1 are implicated in various cancers, including certain gliomas, affecting the PI3K signaling pathway and contributing to abnormal cell growth and survival.
11.	FUBP1	Increase in Low grade glioma	FUBP1, or Far Upstream Element Binding Protein 1, is a gene involved in RNA processing and transcriptional regulation. Mutations and dysregulation of FUBP1 have been implicated in certain cancers, including gliomas, influencing cellular processes and contributing to tumor development.
12.	RB1	Increase in Low grade glioma	RB1, or Retinoblastoma Protein 1, is a tumor suppressor gene regulating the cell cycle. Mutations in RB1 are associated with various cancers, including certain gliomas, impacting cell cycle control and contributing to tumorigenesis.
13.	NOTCH1	Increase in Glioblastoma Multiforme	NOTCH1, a gene in the Notch signalling pathway, plays a crucial role in cellular communication and differentiation. Dysregulation of NOTCH1 is implicated in various cancers, and in gliomas, it may influence cell fate determination and contribute to tumor development.
14.	BCOR	Decrease in Glioblastoma Multiforme	BCOR, or BCL6 Corepressor, is a gene involved in transcriptional regulation. Mutations in BCOR have been identified in certain cancers, including gliomas, potentially impacting cellular processes and contributing to the molecular profile of these tumors.
15.	CSMD3	Increase in Low grade glioma	CSMD3, or CUB and Sushi Multiple Domains 3, is a gene encoding a protein with multiple domains. Alterations in CSMD3 have been associated with various cancers, and in gliomas, these changes may influence cellular processes and contribute to the development of the tumor.
16.	SMARCA4	Increase in Low grade glioma	SMARCA4, or SWI/SNF Related, Matrix Associated, Actin Dependent Regulator of Chromatin, Subfamily A, Member 4, is a gene encoding a key component of the SWI/SNF chromatin remodeling complex. Mutations in SMARCA4 are implicated in various cancers, including certain gliomas, affecting chromatin structure and contributing to tumor development.

TABLE 7. (Continued.) An overview of markers used to predict glioma.

17.	GRIN2A	Decrease in Glioblastoma Multiforme	GRIN2A, or Glutamate Ionotropic Receptor NMDA Type Subunit 2A, is a gene encoding a subunit of the NMDA receptor. Mutations in GRIN2A have been associated with various neurological disorders, and in gliomas, alterations in this gene may impact cellular processes and contribute to the molecular characteristics of the tumor.
18.	IDH2	Increase in Glioblastoma Multiforme	IDH2, or Isocitrate Dehydrogenase 2, is a gene encoding a metabolic enzyme. Mutations in IDH2 are found in certain gliomas, influencing the tumor's molecular characteristics and prognosis similar to IDH1 mutations.
19.	FAT4	Decrease in Glioblastoma Multiforme	FAT4, or FAT Atypical Cadherin 4, is a gene involved in cell adhesion and tissue development. Alterations in FAT4 have been implicated in various cancers, and in gliomas, changes in this gene may impact cellular processes and contribute to the development of the tumor.
20.	PDGFRA	Increase in Glioblastoma Multiforme	PDGFRA, or Platelet-Derived Growth Factor Receptor Alpha, is a gene encoding a cell surface receptor. Amplifications and mutations in PDGFRA are observed in certain gliomas, influencing cell proliferation and contributing to the pathogenesis of these brain tumors.

TABLE 8. Comparative analysis between our proposed methodology and existing approaches.

Sr. No	Model	Classifiers	AUC	Precision	Recall	F1-score	MCC	Explainable AI Techniques
1.	[57]	Complement naive Bayes (CNB), SVM, KNN, Random Forest and artificial neural network (ANN)	0.724	0.794	0.655	NA	0.453	No
2.	[58]	Support vector machine, Multi-layer perceptron classifier	0.986	0.944	NA	NA	NA	No
3.	[59]	eXtreme Gradient Boosting classifier	0.912	0.778	0.778	0.778	NA	No
4.	[60]	Random Forest	0.87	0.65	0.79	NA	NA	No
5.	Proposed model	Random forests, KNN, Logistic regression, Decision trees, SVM (Linear, sigmoid), XgBoost, AdaBoost, CatBoost, LGBM and Stacking models	0.92	0.82	0.94	0.88	0.757	SHAP, Qlattice, ELI5, LIME

*NA-Not Available

VI. LIMITATIONS AND FUTURE SCOPE

A. LIMITATIONS

The quality and availability of the datasets determine how well the model performs, so it is necessary to continuously expand and improve it. Thorough testing, scalability assessments, and external validations are essential before implementing in healthcare institutions in order to guarantee robustness across a variety of clinical settings.

Given the intrinsic complexity of glioma prognosis, careful interpretation of the model's predictions is necessary even with Explainable AI for interpretability. Throughout real-world implementation, ethical issues, patient privacy, and regulatory compliance are critical and require constant attention. These elements highlight how crucial it is to translate our research into useful therapeutic applications using a methodical and cautious approach.

B. FUTURE SCOPE

The future direction of our proposed study involves an integrated approach to enhance the glioma prediction model. We will focus on incorporating advanced features,

continuously expanding the dataset through collaborations with diverse medical institutions worldwide, and integrating the latest imaging modalities. Leveraging state-of-the-art deep learning algorithms and transfer learning techniques will be pivotal, especially when dealing with large datasets. Additionally, international collaboration can be sought to combine data from different countries, creating a globally representative initiative for glioma research. Implementing a cloud-based system will facilitate scalability and collaboration across geographical boundaries. Rigorous medical validation and clinical trials will be conducted, and educational programs will bridge the knowledge gap between informatics and medical experts. Ethical considerations, including patient privacy and data security, will remain paramount throughout the study. This holistic approach aims to not only advance the field of glioma prediction but also provide a valuable tool equally beneficial to both medical professionals and machine learning experts.

VII. CONCLUSION

Early detection and treatment of glioma tumours can improve their prognosis and reduce their risk of consequences. Thus,

we used machine learning and XAI techniques to predict glioma, which was classified as Low-Grade Glioma (LGG) or Glioblastoma Multiforme (GBM) based upon the histology and the criteria for imaging. Beyond enhancing transparency, interpretability (XAI) acts as a bridge between the technical intricacies of machine learning models and real-world decision-makers. It empowers individuals to navigate complex predictions, fostering a symbiotic relationship between human judgment and AI capabilities while addressing regulatory, ethical, and practical considerations. This study's data set comprised 889 patients with 23 features. The three feature selection techniques that were used were mutual information, Pearson's correlation, and the Principal Component Analysis (PCA) algorithm. The XgBoost model reached a maximum accuracy of 88%, while the stacked model attained 82% accuracy. For interpreting the model's predictions, four XAI techniques were used i.e., SHAP, QLattice, Eli5 and LIME.

The most important factors for the prediction of glioma were determined to be IDH1, age at diagnosis, PIK3CA, ATRX, PTEN, CIC, EGFR, and TP53. Furthermore, the efficacy of creating classifier dependability was evaluated by contrasting the suggested method with other relevant studies. These classifiers/models can be utilized by the medical professionals as a decision support system to predict gliomas. An interface might be used to implement real-time prediction of glioma tumour screening; therefore, a broader population's glioma could be predicted using this methodology.

ACKNOWLEDGMENT

The authors would like to thank Manipal Academy of Higher Education for providing computation laboratories.

REFERENCES

- [1] F. B. Mesfin and M. A. Al-Dahir, "Gliomas," in *StatPearls. Treasure Island*, StatPearls. [Online]. Available: <https://www.ncbi.nlm.nih.gov/books/NBK441874/>
- [2] GLIOMA. Accessed: Oct. 8, 2023. [Online]. Available: <https://www.mayoclinic.org/diseases-conditions/glioma/symptoms-causes/syc-20350251>
- [3] Accessed: Oct. 8, 2023. [Online]. Available: <https://www.cancerresearchuk.org/about-cancer/brain-tumours/types/glioma-adults>
- [4] D. N. Louis, H. Ohgaki, O. D. Wiestler, W. K. Cavenee, P. C. Burger, A. Jouvet, B. W. Scheithauer, and P. Kleihues, "The 2007 WHO classification of tumours of the central nervous system," *Acta Neuropathologica*, vol. 114, no. 5, p. 547, Oct. 2007.
- [5] A. Finch, G. Solomou, V. Wykes, U. Pohl, C. Bardella, and C. Watts, "Advances in research of adult gliomas," *Int. J. Mol. Sci.*, vol. 22, no. 2, p. 924, Jan. 2021.
- [6] S. Chatterjee, F. A. Nizamani, A. Nürnberg, and O. Speck, "Classification of brain tumours in MR images using deep spatiotemporal models," *Sci. Rep.*, vol. 12, no. 1, p. 1505, Jan. 2022.
- [7] K. Lenting, R. Verhaak, M. ter Laan, P. Wesseling, and W. Leenders, "Glioma: Experimental models and reality," *Acta Neuropathologica*, vol. 133, no. 2, pp. 263–282, Feb. 2017.
- [8] R. Gupta, S. Flanagan, C. C. Li, M. Lee, B. Shivalingham, S. Maleki, H. R. Wheeler, and M. E. Buckland, "Expanding the spectrum of IDH1 mutations in gliomas," *Modern Pathol.*, vol. 26, no. 5, pp. 619–625, May 2013.
- [9] K. Penne, C. Bohlin, S. Schneider, and D. Allen, "Gefitinib (IressaTM, ZD1839) and tyrosine kinase inhibitors: The wave of the future in cancer therapy," *Cancer Nursing*, vol. 28, no. 6, pp. 481–486, Nov. 2005.
- [10] J. Mukherjee, A. Ghosh, A. Ghosh, and S. Chaudhuri, "ENU administration causes genomic instability along with single nucleotide polymorphisms in p53 during gliomagenesis: T11TS administration demonstrated in vivo apoptosis of these genetically altered tumor cells," *Cancer Biol. Therapy*, vol. 5, no. 2, pp. 156–164, Feb. 2006.
- [11] R. Gómez-Oliva, S. Domínguez-García, L. Carrascal, J. Abalos-Martínez, R. Pardillo-Díaz, C. Verástegui, C. Castro, P. Nunez-Abades, and N. Geribaldi-Doldán, "Evolution of experimental models in the study of glioblastoma: Toward finding efficient treatments," *Frontiers Oncol.*, vol. 10, Jan. 2021, Art. no. 614295.
- [12] P. Rajpurkar, E. Chen, O. Banerjee, and E. J. Topol, "AI in health and medicine," *Nature Med.*, vol. 28, no. 1, pp. 31–38, Jan. 2022.
- [13] B. Mohanta, P. Das, and S. Patnaik, "Healthcare 5.0: A paradigm shift in digital healthcare system using artificial intelligence, IoT and 5G communication," in *Proc. Int. Conf. Appl. Mach. Learn. (ICAML)*, Bhubaneswar, India, May 2019, pp. 191–196.
- [14] R. Bhardwaj, A. R. Nambiar, and D. Dutta, "A study of machine learning in healthcare," in *Proc. IEEE 41st Annu. Comput. Softw. Appl. Conf. (COMPSAC)*, vol. 2, Turin, Italy, Jul. 2017, pp. 236–241.
- [15] D. Saraswat, P. Bhattacharya, A. Verma, V. K. Prasad, S. Tanwar, G. Sharma, P. N. Bokoro, and R. Sharma, "Explainable AI for Healthcare 5.0: Opportunities and challenges," *IEEE Access*, vol. 10, pp. 84486–84517, 2022.
- [16] A. Raza, J. Uddin, A. Almuhaimeed, S. Akbar, Q. Zou, and A. Ahmad, "AIPs-SnTCN: Predicting anti-inflammatory peptides using fastText and transformer encoder-based hybrid word embedding with self-normalized temporal convolutional networks," *J. Chem. Inf. Model.*, vol. 63, no. 21, pp. 6537–6554, Nov. 2023.
- [17] S. Akbar, A. Raza, T. A. Shloul, A. Ahmad, A. Saeed, Y. Y. Ghadi, O. Mamyrbayev, and E. Tag-Eldin, "PAtbP-EnC: Identifying anti-tubercular peptides using multi-feature representation and genetic algorithm-based deep ensemble model," *IEEE Access*, vol. 11, pp. 137099–137114, 2023.
- [18] S. Akbar, M. Hayat, M. Tahir, S. Khan, and F. K. Alarfaj, "CACP-DeepGram: Classification of anticancer peptides via deep neural network and skip-gram-based word embedding model," *Artif. Intell. Med.*, vol. 131, Sep. 2022, Art. no. 102349.
- [19] S. Akbar, M. Hayat, M. Iqbal, and M. A. Jan, "IACP-GAEnsC: Evolutionary genetic algorithm based ensemble classification of anticancer peptides by utilizing hybrid feature space," *Artif. Intell. Med.*, vol. 79, pp. 62–70, Jun. 2017.
- [20] S. Akbar, S. Khan, F. Ali, M. Hayat, M. Qasim, and S. Gul, "IHBP-DeepPSSM: Identifying hormone binding proteins using PsePSSM based evolutionary features and deep learning approach," *Chemometric Intell. Lab. Syst.*, vol. 204, Sep. 2020, Art. no. 104103.
- [21] S. Akbar, H. G. Mohamed, H. Ali, A. Saeed, A. A. Khan, S. Gul, A. Ahmad, F. Ali, Y. Y. Ghadi, and M. Assam, "Identifying neuropeptides via evolutionary and sequential based multi-perspective descriptors by incorporation with ensemble classification strategy," *IEEE Access*, vol. 11, pp. 49024–49034, 2023.
- [22] U. Pawar, D. O'Shea, S. Rea, and R. O'Reilly, "Incorporating explainable artificial intelligence (XAI) to aid the understanding of machine learning in the healthcare domain," in *Proc. AICS*, 2020, pp. 169–180.
- [23] H. Ouerghi, O. Mourali, and E. Zagrouba, "Glioma classification via MR images radiomics analysis," *Vis. Comput.*, vol. 38, no. 4, pp. 1427–1441, Apr. 2022.
- [24] Q. Tian, L. Yan, X. Zhang, X. Zhang, Y. Hu, Y. Han, Z. Liu, H. Nan, Q. Sun, Y. Sun, Y. Yang, Y. Yu, J. Zhang, B. Hu, G. Xiao, P. Chen, S. Tian, J. Xu, W. Wang, and G. Cui, "Radiomics strategy for glioma grading using texture features from multiparametric MRI," *J. Magn. Reson. Imag.*, vol. 48, no. 6, pp. 1518–1528, Dec. 2018.
- [25] H. Cho, S. Lee, J. Kim, and H. Park, "Classification of the glioma grading using radiomics analysis," *PeerJ*, vol. 6, p. e5982, Nov. 2018.
- [26] Y. Wu, B. Liu, W. Wu, Y. Lin, C. Yang, and M. Wang, "Grading glioma by radiomics with feature selection based on mutual information," *J. Ambient Intell. Humanized Comput.*, vol. 9, no. 5, pp. 1671–1682, Oct. 2018.
- [27] H. Cao, E. Z. Erson-Omay, X. Li, M. Günel, J. Moliterno, and R. K. Fulbright, "A quantitative model based on clinically relevant MRI features differentiates lower grade gliomas and glioblastoma," *Eur. Radiol.*, vol. 30, no. 6, pp. 3073–3082, Jun. 2020.
- [28] S. Rathore, T. Niazi, M. A. Iftikhar, and A. Chaddad, "Glioma grading via analysis of digital pathology images using machine learning," *Cancers*, vol. 12, no. 3, p. 578, Mar. 2020.

- [29] K. E. Emblem, F. G. Zoellner, B. Tennoe, B. Nedregard, T. Nome, P. Due-Tonnessen, J. K. Hald, D. Scheie, and A. Bjørnerud, "Predictive modeling in glioma grading from MR perfusion images using support vector machines," *Magn. Reson. Med.*, vol. 60, no. 4, pp. 945–952, Oct. 2008.
- [30] E. I. Zacharakis, S. Wang, S. Chawla, D. Soo Yoo, R. Wolf, E. R. Melhem, and C. Davatzikos, "Classification of brain tumor type and grade using MRI texture and shape in a machine learning scheme," *Magn. Reson. Med.*, vol. 62, no. 6, pp. 1609–1618, Dec. 2009.
- [31] K. L.-C. Hsieh, C.-M. Lo, and C.-J. Hsiao, "Computer-aided grading of gliomas based on local and global MRI features," *Comput. Methods Programs Biomed.*, vol. 139, pp. 31–38, Feb. 2017.
- [32] M. M. Subashini, S. K. Sahoo, V. Sunil, and S. Easwaran, "A non-invasive methodology for the grade identification of astrocytoma using image processing and artificial intelligence techniques," *Expert Syst. Appl.*, vol. 43, pp. 186–196, Jan. 2016.
- [33] W. Chen, B. Liu, S. Peng, J. Sun, and X. Qiao, "Computer-aided grading of gliomas combining automatic segmentation and radiomics," *Int. J. Biomed. Imag.*, vol. 2018, pp. 1–11, Jan. 2018.
- [34] M. Gupta, V. Rajagopalan, and P. Rao, "Glioma grade classification using wavelet transform-local binary pattern based statistical texture features and geometric measures extracted from MRI," *J. Experim. Theor. Artif. Intell.*, vol. 31, no. 1, pp. 57–76, Jan. 2019.
- [35] X. Wang, D. Wang, Z. Yao, B. Xin, B. Wang, C. Lan, Y. Qin, S. Xu, D. He, and Y. Liu, "Machine learning models for multiparametric glioma grading with quantitative result interpretations," *Frontiers Neurosci.*, vol. 12, pp. 1–11, Jan. 2019, Art. no. 1046.
- [36] Y. Yang, L. Yan, X. Zhang, H. Nan, Y. Hu, Y. Han, J. Zhang, Z. Liu, Y. Sun, Q. Tian, Y. Yu, Q. Sun, S. Wang, X. Zhang, W. Wang, and G. Cui, "Optimizing texture retrieving model for multimodal MR image-based support vector machine for classifying glioma," *J. Magn. Reson. Imag.*, vol. 49, no. 5, pp. 1263–1274, May 2019.
- [37] Z. Lu, Y. Bai, Y. Chen, C. Su, S. Lu, T. Zhan, X. Hong, and S. Wang, "The classification of gliomas based on a pyramid dilated convolution resnet model," *Pattern Recognit. Lett.*, vol. 133, pp. 173–179, May 2020.
- [38] J. Jeong, L. Wang, B. Ji, Y. Lei, A. Ali, T. Liu, W. J. Curran, H. Mao, and X. Yang, "Machine-learning based classification of glioblastoma using delta-radiomic features derived from dynamic susceptibility contrast enhanced magnetic resonance images," *Quant. Imag. Med. Surgery*, vol. 9, no. 7, pp. 1201–1213, Jul. 2019.
- [39] E. Tasci, K. Camphausen, A. V. Krauze, and Y. Zhuge, "Glioma grading clinical and mutation features dataset," UC Irvine Mach. Learn. Repository California, Tech. Rep., 2020, doi: [10.24432/C5R62J](https://doi.org/10.24432/C5R62J).
- [40] D. Tanasa and B. Trousselle, "Advanced data preprocessing for intersites web usage mining," *IEEE Intell. Syst.*, vol. 19, no. 2, pp. 59–65, Mar. 2004.
- [41] V. V. Khanna, K. Chadaga, N. Sampathila, S. Prabhu, V. Bhandage, and G. K. Hegde, "A distinctive explainable machine learning framework for detection of polycystic ovary syndrome," *Appl. Syst. Innov.*, vol. 6, no. 2, p. 32, Feb. 2023.
- [42] H. Han, W. Y. Wang, and B. H. Mao, "Borderline-SMOTE: A new oversampling method in imbalanced data sets learning," in *Proc. Int. Conf. Intell. Comput.*, Hefei, China. Berlin, Germany: Springer, Aug. 2005, pp. 878–887.
- [43] K. Potdar, T. Pardawala, and C. Pai, "A comparative study of categorical variable encoding techniques for neural network classifiers," *Int. J. Comput. Appl.*, vol. 175, no. 4, pp. 7–9, Oct. 2017.
- [44] P. Ahlgren, B. Jarneving, and R. Rousseau, "Requirements for a cocitation similarity measure, with special reference to Pearson's correlation coefficient," *J. Amer. Soc. Inf. Sci. Technol.*, vol. 54, no. 6, pp. 550–560, Apr. 2003.
- [45] A. Pradhan, S. Prabhu, K. Chadaga, S. Sengupta, and G. Nath, "Supervised learning models for the preliminary detection of COVID-19 in patients using demographic and epidemiological parameters," *Information*, vol. 13, no. 7, p. 330, Jul. 2022.
- [46] J. R. Vergara and P. A. Estévez, "A review of feature selection methods based on mutual information," *Neural Comput. Appl.*, vol. 24, no. 1, pp. 175–186, Jan. 2014.
- [47] T. Kurita, "Principal component analysis (PCA)," in *Computer Vision: A Reference Guide*. Cham, Switzerland: Springer, 2019, pp. 1–4.
- [48] B. M. S. Hasan and A. M. Abdulazeez, "A review of principal component analysis algorithm for dimensionality reduction," *J. Soft Comput. Data Mining*, vol. 2, no. 1, pp. 20–30, 2021.
- [49] C. Labrin and F. Urdinez, "Principal component analysis," in *R for Political Data Science*. London, U.K.: Chapman & Hall, 2020, pp. 375–393.
- [50] H. J. P. Weerts, A. C. Mueller, and J. Vanschoren, "Importance of tuning hyperparameters of machine learning algorithms," 2020, *arXiv:2007.07588*.
- [51] *Stacking in Machine Learning-Javatpoint*. Accessed: Oct. 5, 2023. [Online]. Available: <https://www.javatpoint.com/stacking-in-machine-learning>
- [52] Y. LeCun, Y. Bengio, and G. Hinton, "Deep learning," *Nature*, vol. 521, no. 7553, pp. 436–444, 2015.
- [53] K. O'Shea and R. Nash, "An introduction to convolutional neural networks," 2015, *arXiv:1511.08458*.
- [54] L. Alzubaidi, J. Zhang, A. J. Humaidi, A. Al-Dujaili, Y. Duan, O. Al-Shamma, J. Santamaría, M. A. Fadhel, M. Al-Amidie, and L. Farhan, "Review of deep learning: Concepts, CNN architectures, challenges, applications, future directions," *J. Big Data*, vol. 8, no. 1, p. 53, Mar. 2021.
- [55] R. Yamashita, M. Nishio, R. K. G. Do, and K. Togashi, "Convolutional neural networks: An overview and application in radiology," *Insights into Imag.*, vol. 9, no. 4, pp. 611–629, Aug. 2018.
- [56] Z. Li, F. Liu, W. Yang, S. Peng, and J. Zhou, "A survey of convolutional neural networks: Analysis, applications, and prospects," *IEEE Trans. Neural Netw. Learn. Syst.*, vol. 33, no. 12, pp. 6999–7019, Dec. 2022.
- [57] P. Korica, N. E. Gayar, and W. Pang, "Explainable artificial intelligence in healthcare: Opportunities, gaps and challenges and a novel way to look at the problem space," in *Proc. 22nd Int. Conf. Intell. Data Eng. Automated Learn.*, Manchester, U.K. Cham, Switzerland: Springer, 2021, pp. 333–342.
- [58] K. Chadaga, S. Prabhu, N. Sampathila, and R. Chadaga, "A machine learning and explainable artificial intelligence approach for predicting the efficacy of hematopoietic stem cell transplant in pediatric patients," *Healthcare Anal.*, vol. 3, Nov. 2023, Art. no. 100170.
- [59] M. J. Raihan, M. A.-M. Khan, S.-H. Kee, and A.-A. Nahid, "Detection of the chronic kidney disease using XGBoost classifier and explaining the influence of the attributes on the model using SHAP," *Sci. Rep.*, vol. 13, no. 1, p. 6263, Apr. 2023.
- [60] M. Bhandari, P. Yogarajah, M. S. Kavitha, and J. Condell, "Exploring the capabilities of a lightweight CNN model in accurately identifying renal abnormalities: Cysts, stones, and tumors, using LIME and SHAP," *Appl. Sci.*, vol. 13, no. 5, p. 3125, Feb. 2023.
- [61] M. S. Islam, I. Hussain, M. M. Rahman, S. J. Park, and M. A. Hossain, "Explainable artificial intelligence model for stroke prediction using EEG signal," *Sensors*, vol. 22, no. 24, p. 9859, Dec. 2022.
- [62] K. Chadaga, S. Prabhu, V. Bhat, N. Sampathila, S. Umakanth, and R. Chadaga, "A decision support system for diagnosis of COVID-19 from non—COVID-19 influenza-like illness using explainable artificial intelligence," *Bioengineering*, vol. 10, no. 4, p. 439, Mar. 2023.
- [63] A. B. Parsa, A. Movahedi, H. Taghipour, S. Derrible, and A. Mohammadian, "Toward safer highways, application of XGBoost and SHAP for real-time accident detection and feature analysis," *Accident Anal. Prevention*, vol. 136, Mar. 2020, Art. no. 105405.
- [64] K. E. Mokhtari, B. P. Higdon, and A. Başar, "Interpreting financial time series with SHAP values," in *Proc. 29th Annu. Int. Conf. Comput. Sci. Softw. Eng.*, Markham, ON, Canada, Nov. 2019, pp. 166–172.
- [65] M. R. Zafar and N. Khan, "Deterministic local interpretable model-agnostic explanations for stable explainability," *Mach. Learn. Knowl. Extraction*, vol. 3, no. 3, pp. 525–541, Jun. 2021.
- [66] N. B. Kumarakulasringhe, T. Blomberg, J. Liu, A. S. Leao, and P. Papapetrou, "Evaluating local interpretable model-agnostic explanations on clinical machine learning classification models," in *Proc. IEEE 33rd Int. Symp. Comput.-Based Med. Syst. (CBMS)*, Rochester, MN, USA, Jul. 2020, pp. 7–12.
- [67] P. A. Riyantoko, Sugiarto, I. G. S. M. Diyasa, and Kraugusteeliana, "F.Q.A.M' FEYN-QLattice automation modelling: Python module of machine learning for data classification in water potability," in *Proc. Int. Conf. Informat., Multimedia, Cyber Inf. Syst. (ICIMCIS)*, Oct. 2021, pp. 135–141.
- [68] P. Purwono, A. Ma'arif, I. S. M. Negara, W. Rahmiani, and J. Rahmawan, "Linkage detection of features that cause stroke using feyn qlattice machine learning model," *Jurnal Ilmiah Teknik Elektro Komputer dan Informatika*, vol. 7, no. 3, p. 423, Dec. 2021.
- [69] S. Kawakura, M. Hirafuji, S. Ninomiya, and R. Shibasaki, "Adaptations of explainable artificial intelligence (XAI) to agricultural data models with ELIS, PDPbox, and skater using diverse agricultural worker data," *Eur. J. Artif. Intell. Mach. Learn.*, vol. 1, no. 3, pp. 27–34, Dec. 2022.

- [70] Y. Jiang and L. Uhrbom, "On the origin of glioma," *Upsala J. Med. Sci.*, vol. 117, no. 2, pp. 113–121, May 2012.
- [71] R. Chai, S. Fang, B. Pang, Y. Liu, Y. Wang, W. Zhang, and T. Jiang, "Molecular pathology and clinical implications of diffuse glioma," *Chin. Med. J.*, vol. 135, no. 24, pp. 2914–2925, Dec. 2022.
- [72] F. Hanif, K. Muzaffar, K. Perveen, S. M. Malhi, and S. U. Simjee, "Glioblastoma multiforme: A review of its epidemiology and pathogenesis through clinical presentation and treatment," *Asian Pacific J. Cancer Prevention*, vol. 18, no. 1, pp. 3–9, Jan. 2017, doi: 10.22034/APJCP.2017.18.1.3.
- [73] H. Yan, D. W. Parsons, G. Jin, R. McLendon, B. A. Rasheed, W. Yuan, and D. D. Bigner, "IDH1 and IDH2 mutations in gliomas," *New England J. Med.*, vol. 360, no. 8, pp. 765–773, 2009.
- [74] J. E. Eckel-Passow et al., "Glioma groups based on 1p/19q, IDH, and TERT promoter mutations in tumors," *New England J. Med.*, vol. 372, no. 26, pp. 2499–2508, 2015.
- [75] B. Niu, C. Liang, Y. Lu, M. Zhao, Q. Chen, Y. Zhang, L. Zheng, and K.-C. Chou, "Glioma stages prediction based on machine learning algorithm combined with Protein-Protein interaction networks," *Genomics*, vol. 112, no. 1, pp. 837–847, Jan. 2020.
- [76] P. Sun, D. Wang, V. C. Mok, and L. Shi, "Comparison of feature selection methods and machine learning classifiers for radiomics analysis in glioma grading," *IEEE Access*, vol. 7, pp. 102010–102020, 2019.
- [77] K. R. Bhatele and S. S. Bhadauria, "Machine learning application in glioma classification: Review and comparison analysis," *Arch. Comput. Methods Eng.*, vol. 29, no. 1, pp. 247–274, Jan. 2022.
- [78] C. H. Sudre et al., "Machine learning assisted DSC-MRI radiomics as a tool for glioma classification by grade and mutation status," *BMC Med. Informat. Decis. Making*, vol. 20, no. 1, Dec. 2020.



ANISHA PALKAR received the B.E. degree from the Department of Biomedical Engineering, Mahatma Gandhi Mission College of Engineering and Technology (MGMCET), Mumbai, University of Mumbai. She is currently pursuing the master's (M.Tech.) degree in medical informatics with the Department of Biomedical Engineering, Manipal Institute of Technology, Manipal. She has presented research papers in two international conferences (IEEE and ICCMEH). She has published a review article in *Journal of BMESI*, a research article in IEEE Xplore, and has keen interest in research for classification and prediction task of diseases.



CIFHA CRECIL DIAS (Senior Member, IEEE) received the B.E. degree in electrical and electronics engineering, the M.Tech. degree in control systems, and the Ph.D. degree from the Department of Instrumentation and Control Engineering, Manipal Institute of Technology, Manipal. She is currently an Assistant Professor (Senior Scale) with the Department of Biomedical Engineering, Manipal Institute of Technology. Her research interests include precision control in drug delivery, AI and ML, biomedical control and signal, sensor monitoring and medical device, and disease diagnosis prediction. She has ten years of teaching and four years of research experience. She has published articles in reputed journals and has been an active reviewer in various journals.



KRISHNARAJ CHADAGA received the B.E. degree from the Department of Computer Science and Engineering, Shri Madwadairaja Institute of Technology, and the M.Tech. degree from Manipal Institute of Technology, Manipal. He is currently a Research Scholar with the Department of Computer Science and Engineering, Manipal Institute of Technology. He has already published articles in reputed journals and has been an active reviewer. His research interests include medical informatics, disease classification, decision support management systems, and disease diagnosis/prognosis prediction.



NIRANJANA SAMPATHILA (Senior Member, IEEE) received the B.E. degree in electronics and engineering and the M.Tech. degree in biomedical engineering from Mangalore University and the Ph.D. degree from Manipal University (currently known as Manipal Academy of Higher Education), Manipal, India. He is currently a Professor with the Department of Biomedical Engineering, Manipal Institute of Technology, Manipal Academy of Higher Education. He has more than 26 years of experience in research and academics in healthcare applications/biomedical engineering/electronics and communication engineering. He has published a good number of papers in journals and conferences. His research interests include pattern recognition, medical informatics, miniaturized system design, nanoelectronics, and AI for healthcare. He is a fellow of IE (India).